Supplementary Materials

Morphology of dome- and tepee-like landforms generated by expansive hydration of weathering anhydrite: a case study at Dingwall, Nova Scotia, Canada.

Adrian Jarzyna, Maciej Bąbel, Damian Ługowski, Firouz Vladi

Applied Sciences ***2022****, 12*

Table S1: Inventory of hydration landforms with basic morphometric parameters and GPS locations.

Figure S1: Applied photogrammetric method – equipment, course of work and results.

Figure S2: Hydration landforms on the orthophotomaps and digital surface models.

Figure S3: Location of hydration landforms on the basemap of satellite image with characteristic of their sizes.

Figure S4: Location of hydration landforms with measured thickness of the detached layer on the basemap of satellite image.

Figure S5: Frequency distribution diagrams of morphometric parameters characterising hydration landforms.

Figure S6: Dependence of relative height of hydration landforms on length, width, bulge degree and coefficient of circularity.

Figure S7: Pattern of fractures within hydration forms.

Figure S8: Traces of fractures and rock layers on the orthophotomaps of the quarry bottom.

Figure S9: Exemplary hydration landforms influenced by structural types of bedrock.

Supplementary material to the paper: Jarzyna A., Bąbel M., Ługowski D., Vladi F. 2022. Morphology of dome- and tepee-like landforms generated by expansive hydration of weathering anhydrite: a case study at Dingwall, Nova Scotia, Canada. In: Geomorphology in the Digital Era. A. Muzirafuti, G. Randazzo, S. Lanza (Eds.), Special Issue of Applied Sciences.

Table S1

Inventory of hydration forms at Dingwall

No. of hydration form	Length a [m]	Width b [m]	Relative height h_r [m]	Thickness of layer e [m]	Mean elevation [m n.p.m.]	Fracture density F_D [m/m^2]	Circularity coefficient (a-b)/a	Bulge degree b/h_r	GPS coordinates
1	7.06	4.96	1.34	0.27	29.34	0.11	0.30	3.70	60°28'58.725"W 46°53'31.238"N
2	2.11	1.55	0.57	0.17	29.23	0.10	0.27	2.71	60°28'58.859"W 46°53'31.285"N
3	13.32	3.63	0.86	0.20	28.52	0.04	0.73	4.21	60°28'58.418"W 46°53'31.773"N
4	7.61	5.60	1.03	0.12	28.63	0.87	0.26	5.44	60°28'58.988"W 46°53'31.731"N
5	6.77	3.90	1.07	0.18	30.28	2.07	0.42	3.64	60°28'59.703"W 46°53'31.742"N
6	11.07	9.01	1.46	0.35	34.83	0.25	0.19	6.17	60°29'1.767"W 46°53'33.819"N
7	6.47	3.49	1.09	0.30	33.65	0.64	irregular	3.20	60°29'1.107"W 46°53'33.177"N
8	7.10	5.23	0.77	0.20	34.58	0.06	0.26	6.83	60°29'1.608"W 46°53'34.167"N
9	5.66	3.72	0.61	0.20	34.09	0.31	0.34	6.12	60°29'0.441"W 46°53'34.371"N
10	4.93	2.39	0.48	0.15*	33.99	0.15	0.52	5.01	60°29'0.613"W 46°53'34.37"N
11	5.50	2.80	0.55	0.15*	34.02	0.31	0.49	5.09	60°29'0.713"W 46°53'34.373"N
12	3.50	2.23	0.33	0.15*	33.67	2.42	0.36	6.82	60°29'0.754"W 46°53'34.543"N
13	4.72	2.97	0.77	0.15*	34.24	0.20	0.37	3.86	60°29'0.024"W 46°53'33.961"N
14	4.74	4.56	0.93	0.20*	29.38	0.69	0.04	4.90	60°28'59.084"W 46°53'33.117"N
15	6.80	2.96	1.62	0.43	33.00	1.46	0.56	1.82	60°28'59.446"W 46°53'35.087"N
16	2.64	2.27	0.48	0.06	29.32	2.88	0.14	4.73	60°28'59.4"W 46°53'32.567"N
17	23.05	8.02	2.08	0.30*	30.30	0.91	0.65	3.86	60°28'59.831"W 46°53'32.267"N
18	3.02	2.13	0.55	0.20	32.77	1.68	0.29	3.87	60°29'0.986"W 46°53'32.841"N
19	4.17	2.12	0.70	0.20*	32.63	0.25	irregular	3.04	60°29'0.665"W 46°53'33.15"N
20	4.10	2.21	0.72	0.20	30.41	2.16	0.46	3.07	60°28'59.915"W 46°53'32.142"N
21	2.88	2.27	0.50	0.20	30.85	0.73	0.21	4.54	60°29'0.032"W 46°53'32.003"N
22	6.12	4.25	0.80	0.40*	32.69	0.05	0.31	5.32	60°28'59.119"W 46°53'34.809"N
23	5.72	4.46	1.30	0.31	25.13	1.66	0.22	3.44	60°28'56.619"W 46°53'32.977"N
24	9.76	4.98	1.69	0.35	37.36	0.64	0.49	2.95	60°29'8.278"W 46°53'39.345"N
25	3.14	2.61	0.66	0.30*	38.15	0.31	0.17	3.96	60°29'7.942"W 46°53'39.671"N
26	5.91	4.68	1.25	0.40	37.37	0.12	0.21	3.75	60°29'7.535"W 46°53'39.389"N
27	5.66	2.74	0.99	0.20*	37.76	0.89	0.52	2.77	60°29'7.673"W 46°53'39.622"N
28	4.17	3.76	0.73	0.25*	38.19	0.42	0.10	5.14	60°29'7.487"W 46°53'39.929"N
29	9.10	7.11	1.05	0.35	43.96	0.05	0.22	6.76	60°29'22.481"W 46°53'34.113"N
30	3.58	2.19	0.40	0.10	44.01	0.00	0.39	5.48	60°29'23.104"W 46°53'34.082"N
31	2.49	1.64	0.33	0.09	43.67	0.57	0.34	4.97	60°29'23.545"W 46°53'33.32"N
32	3.15	2.33	0.61	0.10	43.83	0.56	0.26	3.83	60°29'23.519"W 46°53'33.155"N

Supplementary material to the paper: Jarzyna A., Bąbel M., Ługowski D., Vladi F. 2022. Morphology of dome- and tepee-like landforms generated by expansive hydration of weathering anhydrite: a case study at Dingwall, Nova Scotia, Canada. In: Geomorphology in the Digital Era. A. Muzirafuti, G. Randazzo, S. Lanza (Eds.), Special Issue of Applied Sciences.

		33	4.89	4.11	1.05	0.11	36.38	0.79	0.16	3.91	60°29'24.044"W 46°53'37.534"N
		34	2.95	1.66	0.69	0.33	35.98	0.25	0.44	2.39	60°29'24.194"W 46°53'37.528"N
		35	3.39	1.48	0.51	0.15*	4.43	3.02	0.56	2.92	60°28'25.543"W 46°53'18.001"N
		36	4.89	3.14	0.87	0.10*	3.99	2.19	0.36	3.60	60°28'25.376"W 46°53'17.846"N
		37	1.88	1.64	0.40	0.16	4.78	1.65	0.13	4.10	60°28'26.066"W 46°53'18.232"N
		38	2.20	1.42	0.44	0.13	4.34	2.10	0.35	3.22	60°28'25.157"W 46°53'18.689"N
		39	4.32	3.91	0.91	0.10	5.08	0.26	0.09	4.30	60°28'25.163"W 46°53'18.97"N
		40	4.12	2.59	0.70	0.15	3.54	2.72	0.37	3.69	60°28'24.544"W 46°53'18.604"N
		41	5.58	3.04	0.67	0.30*	3.07	0.28	0.46	4.55	60°28'24.057"W 46°53'18.371"N
		42	3.07	2.06	0.51	0.21	5.69	0.65	0.61	4.04	60°28'22.133"W 46°53'19.715"N
		43	3.07	2.93	0.60	0.15	6.11	0.06	0.05	4.91	60°28'22.48"W 46°53'19.803"N
		44	4.33	3.45	0.66	0.12	5.84	0.25	0.20	5.25	60°28'22.294"W 46°53'19.897"N
		45	5.19	2.10	1.06	0.33	15.15	0.66	0.60	1.98	60°28'58.944"W 46°53'19.082"N
		46	3.74	3.03	0.42	0.09	15.11	0.58	0.19	7.24	60°28'58.761"W 46°53'18.724"N
		47	7.68	6.04	1.04	0.20	14.18	0.24	0.21	5.81	60°28'58.211"W 46°53'18.204"N
		48	4.64	2.33	0.41	0.20	13.77	0.22	0.50	5.65	60°28'57.442"W 46°53'18.657"N
		49	9.49	7.12	2.09	0.46	8.36	0.06	0.25	3.41	60°28'56.971"W 46°53'12.116"N
		50	2.55	1.38	0.48	0.23	11.80	0.40	0.46	2.88	60°28'58.136"W 46°53'13.283"N
		51	2.97	2.66	0.61	0.15	9.87	0.31	0.10	4.36	60°28'57.155"W 46°53'13.917"N
		52	4.58	4.11	0.64	0.20*	8.90	1.13	irregular	6.42	60°28'56.168"W 46°53'14.059"N
		53	5.42	3.93	0.85	0.20	33.37	1.28	irragular	4.92	60°29'1.739"W 46°53'35.557"N
		54	7.09	4.40	1.30	0.23	32.38	1.05	0.38	3.40	60°29'1.745"W 46°53'36.03"N
		55	6.79	4.17	1.36	0.29	35.70	0.59	0.39	3.06	60°29'4.836"W 46°53'36.925"N
		56	3.42	1.76	0.84	0.25	36.62	0.81	0.49	2.10	60°29'10.059"W 46°53'41.282"N
		57	5.00	3.45	1.16	0.28	36.90	0.36	irregular	2.97	60°29'10.268"W 46°53'41.329"N
		58	8.80	4.40	1.20	0.18	38.56	0.00	0.50	3.67	60°29'7.066"W 46°53'39.773"N
		59	5.05	2.65	0.60	0.18	32.82	0.58	0.48	4.42	60°29'1.461"W 46°53'35.57"N
		60	5.77	3.48	0.66	0.18	36.75	0.00	0.40	5.24	60°29'10.73"W 46°53'41.657"N
		61	5.13	3.48	0.58	0.28	36.87	0.40	0.32	5.96	60°29'7.632"W 46°53'39.091"N
		62	4.80	4.35	0.72	0.10	34.99	0.83	0.09	6.04	60°29'7.07"W 46°53'35.754"N
		63	3.49	2.01	0.34	0.10	32.43	1.77	0.42	5.91	60°28'59.406"W 46°53'34.728"N
		64	2.44	2.34	0.58	0.14	26.86	0.35	0.04	4.03	60°29'12.637"W 46°53'48.318"N
		65	3.19	2.19	0.35	0.10*	6.04	0.00	0.31	6.26	60°28'55.29"W 46°53'12.831"N
		66	1.86	0.91	0.35	0.15*	4.19	0.81	0.51	2.61	60°28'25.523"W 46°53'18.306"N
		67	3.06	1.75	0.90	0.15*	3.31	3.38	0.43	1.95	60°28'25.379"W 46°53'17.732"N

Supplementary material to the paper: Jarzyna A., Bąbel M., Ługowski D., Vladi F. 2022. Morphology of dome- and tepee-like landforms generated by expansive hydration of weathering anhydrite: a case study at Dingwall, Nova Scotia, Canada. In: Geomorphology in the Digital Era. A. Muzirafuti, G. Randazzo, S. Lanza (Eds.), Special Issue of Applied Sciences.

68	5.21	4.34	0.51	0.25*	2.93	0.29	irregular	8.58	60°28'21.628"W 46°53'19.213"N
69				0.20*					60°29'1.195"W 46°53'39.296"N
70				0.25*					60°29'3.577"W 46°53'46.89"N
71									60°28'57.724"W 46°53'45.09"N
72	4.55	3.22	0.78	0.30	11.21	0.00	0.29	4.13	60°28'57.331"W 46°53'15.351"N
73	7.08	5.35	1.57	0.24	23.10	1.19	0.24	3.41	60°29'11.654"W 46°53'50.365"N
74	4.83	3.39	1.06	0.26	5.02	0.59	0.30	3.20	60°28'55.187"W 46°53'13.544"N
75	5.16	3.47	0.83	0.12	4.60	0.66	0.33	4.18	60°28'54.993"W 46°53'13.502"N
76	3.05	2.31	0.96	0.20	36.58	0.40	0.24	2.41	60°29'7.284"W 46°53'36.355"N
77	3.78	3.62	1.13	0.10	36.57	1.85	0.04	3.19	60°29'9.764"W 46°53'39.893"N

* - thickness of elevated rock layer measured on photographs and in graphic program Corel Draw

- lack of data
- hydration form documented by 3D or 2.5D model
- hydration form being part of 2.5D model of the quarry
- domed hydration form
- tepee-shaped hydration form

Supplementary material to the paper: Jarzyna A., Bąbel M., Ługowski D., Vladi F. 2022. Morphology of dome- and tepee-like landforms generated by expansive hydration of weathering anhydrite: a case study at Dingwall, Nova Scotia, Canada. In: Geomorphology in the Digital Era. A. Muzirafuti, G. Randazzo, S. Lanza (Eds.), Special Issue of Applied Sciences.

Figure S1

Applied photogrammetric method – equipment, course of work and results.

Documentation of the Dingwall quarry bottom was made using aerial and terrestrial photogrammetry during two expeditions: September 10-26th, 2018 and August 15-29th, 2019. Three photographic devices were used in the field: the UAV (model: DJI Phantom 4 Advanced) and two models of cameras (fig. IB-D; III). In addition, a GPS receiver that supports RTK corrections (Real Time Kinematic) was used, for measuring control and checking points with an accuracy of approx. 1-2 cm (using the NAD_1983_MTM_4 coordinate system). Also, three sizes of portable boards made of PVC material were used to mark the checkpoints on the surface characterized by three sizes: 1) 42×45.5 cm (fig. IA); 2) 14×42 cm; 3) 10×61 cm printed with a unique graphic symbol generated in the Photoscan program. Also on the surface of the quarry bottom, in the case of selected fields, points were spray-painted to check the accuracy of the model fit to the coordinate system.

Fig. I. The selected equipment for the photogrammetry method applied at Dingwall; A – largest portable PCV board 42×45.5 cm used as a control point; B – Unmanned Aerial Vehicle DJI Phantom 4 Advanced; C – Nikon D7100; D – Olympus E-PL 6 Lite.

The UAV flight over the quarry was made with the approval of the Canadian Ministry of Transport. Seven areas were documented within three fields of the quarry (fig. II). Five areas were documented in 2018, two areas in 2019. Before the flight, boards serving as checkpoints (both in 2018 and 2019) and checking points (in 2019) were placed on the surface. The UAV flights for photogrammetric documentation were made at a height of 25 m above the ground. The adjacent photographs were taken with an overlappe of 60-80%. During flight a pilot adjusted the height of 25 m precisely to the topography of the terrain. The flight procedure was performed using the DJI application installed on the mobile device.

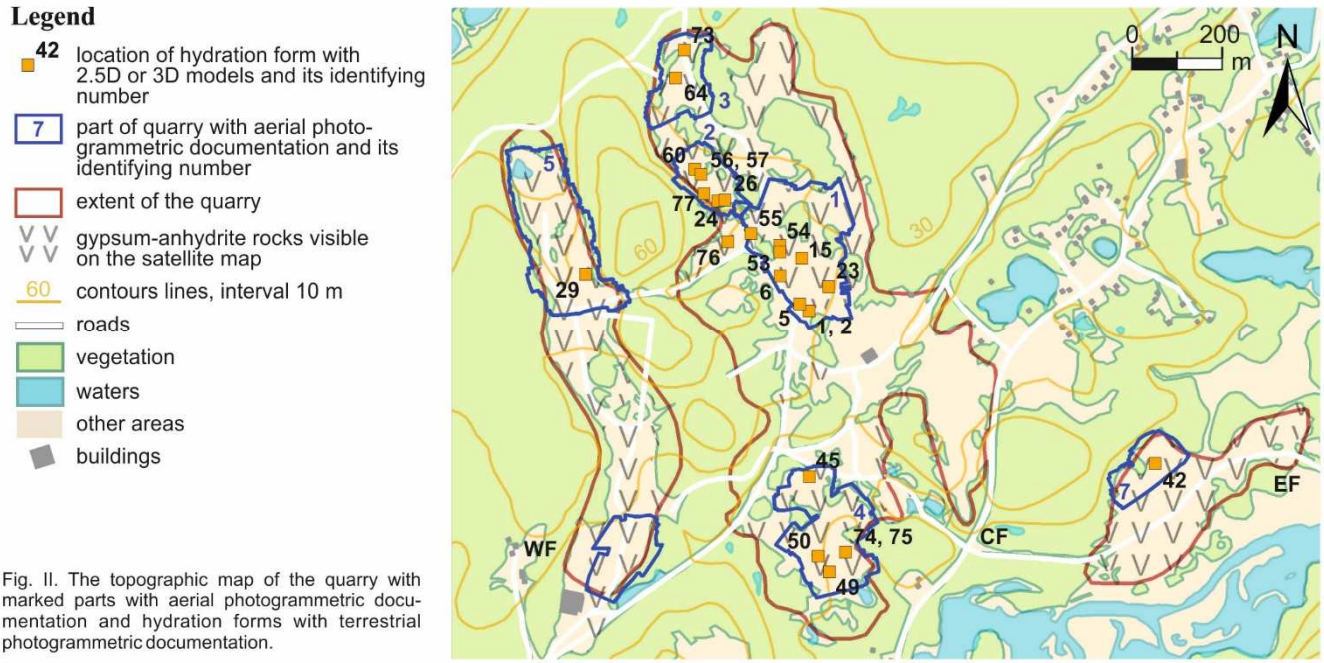

Fig. II. The topographic map of the quarry with marked parts with aerial photogrammetric documentation and hydration forms with terrestrial photogrammetric documentation.

Terrestrial photogrammetric documentation was made for 25 hydration forms in the form of 22 models (3 models include 2 adjacent forms; fig. II). Two selected hydration forms (form no. 1 and no. 6) were documented twice by making their models in 2018 and 2019. The cameras used: Nikon D7100 and Olympus PEN Lite E-PL 6 made it possible to photograph objects in the form of a RAW file, enabling further processing of photographs in a graphic program RawTherapee. The photographs were taken from three different heights located along the lines around the object and inside the cavity. The overlapping of individual shots was preserved in the range of approx. 60-80%. The photographs that needed correction were imported into RawTherapee, where a manual shadow adjustment, exposure correction, and brightening were initiated.

Photographs together with the collected control and checking points and GPS points became the basis for further work in the Photoscan photogrammetry program, based on the Structure from Motion tool (short: SfM), creating an object in 3D on the basis of overlapping photographs (Westoby et al. 2012). The program uses metadata stored in a JPEG image in the form of EXIF (Exchangeable Image File Format) containing information about the camera model, camera settings, shutter speed and focal length (Snavely 2008). SfM uses the Bundle Adjustment algorithm in the object modeling process, enabling the location of the photograph and generation of the geometry of the object in 3D space (Snavely 2008; Triggs et al. 2000).

The methodology of documentary photogrammetric works was described in the previous work of the authors (Jarzyna et al. 2020b) as well as in the instructions for the used program (AgiSoft 2016).

Supplementary material to the paper: Jarzyna A., Bąbel M., Ługowski D., Vladi F. 2022. Morphology of dome- and tepee-like landforms generated by expansive hydration of weathering anhydrite: a case study at Dingwall, Nova Scotia, Canada. In: Geomorphology in the Digital Era. A. Muzirafuti, G. Randazzo, S. Lanza (Eds.), Special Issue of Applied Sciences.

The photogrammetric works resulted in twenty six 3D models of hydration forms covering 0.23 ha and eight 2.5D models of fragments of the quarry area covering 27.55 ha. On the basis of each of them, orthophotomaps and DSMs were created separately with the parameters listed in the table (fig. IV). The average size of the DSM field pixel is 2.54 mm/px for 3D models of hydration forms and 33.60 mm/px for 2.5D models of the quarry bottom. The orthophotomap is characterized by the size of the field pixel at the average value of 0.623 mm/px for 3D models and 2.5D models. The data with above mentioned good quality of image resolution are the basis for further work in the ArcGIS program.

	Maps of study area	3D or 2.5 models
Time of field works	10.09-26.09.2018; 15.08-29.08.2019	
Number of images captured	4388	5138
Number of models	8	24
Area covered (m^2)	275500 m^2	2316 m^2
Ground Sampling Distance of DSM (minimum - maximum; **average value**) [mm]	12.6 - 54.9, **33.6**	1.18 - 8.04; **2.54**
Ground Sampling Distance of orthophotomap (minimum - maximum; **average value**) [mm]	5.45 - 6.87, **6.30**	1.06 - 0.358; **0.623**
Amount of points per cm^2 (minimum - maximum; **average value**)	15 - 415, **211**	2; 72; **26**
Root Square Mean Error for Ground Control Points (minimum - maximum; **average value**; cm)	0.011 - 26.914; **6.03**	0.007 - 48.823; **4.12**
Amount of Ground Control Points (minimum - maximum; **average value**)	4 - 11, **6**	3 - 11; **5**
Root Square Mean Error for Check Points (minimum - maximum; **average value**) [cm]	2.547 - 13.487, **6.64**	2.515 - 1.231; **2.08**
Amount of Check Points (minimum - maximum; **average value**)	11 - 22, **16**	5 - 13; **8**

Fig. IV. Performance data obtained thanks to the photogrammetry method.

	Aerial photogram.	Terrestrial photogrammetry	
Type of photogrammetric equipment	Unmanned Aerial Vehicle	Digital Single Lens Reflex camera	Mirrorless Interchangeable Lens camera
Producer	SZ DJI Technology Co., Ltd.	Nikon Corporation	Olympus Corporation
Model	Phantom 4 Advanced	D7100	PEN Lite E-PL 6
Fixing of camera	non-detachable, 3-axis gimbal	fixed	fixed
Image sensor	1", CMOS, 24 Mpx	APS-C, CMOS, 24 Mpx	4/3", 16.1 Mpx
Focal length	18 mm	18 mm	25 mm
Equivalent of full frame focal length	48.6 mm	27 mm	50 mm
Equivalent type of lens	standard angle	wide angle	standard angle
Shutter release	mobile application DJI GO 4 or controller	—	—
Estimated work time with one battery	30 min	4-5 hours	5-6 hours
Essential software during laboratory works	Agisoft Photoscan Professional		
Additional software during laboratory works	ArcGIS, Agisoft Viewer, Corel Graphic X9, X7, RawTherapee 5.4, Adobe Reader, Microsoft Excel		

Fig. III. Information about equipment and software used in photogrammetric method.

References:

Agisoft. Agisoft PhotoScan User Manual Professional Edition, Version 1.2; Agisoft LLC: St Petersburg, Russia, 2016; 1–97.

Jarzyna, A.; Bąbel, M.; Ługowski, D.; Vladi, F.; Yatsyshyn, A.; Olszewska-Nejbert, D.; Nejbert, K.; Bogucki, A. Unique hydration caves and recommended photogrammetric methods for their documentation. Geoheritage 2020b, 12, 1–15. https://doi.org/10.1007/s12371-020-00425-y

Snavely, K.N. Scene Reconstruction and Visualization from Internet Photo Collections. PhD Thesis, University of Washington, Seattle, USA, 2008; pp. 1–192.

Triggs, B.; Mclauchlan, P.; Hartley, R.; Fitzgibbon, A. Bundle adjustment - a modern synthesis. In Vision Algorithms: Theory and Practice; Triggs, B.; Zisserman, A.; Szeliski, R., Eds.; Springer: Berlin, Heidelberg, 2000; IWVA 1999, Lecture Notes in Computer Science, Volume 1883; pp. 1–71.

Westoby, M.J.; Brasington, J.; Glasser, N.F.; Hambrey, M.J.; Reynolds, J.M. 'Structure-from-motion' photogrammetry: a low-cost, effective tool for geoscience applications. Geomorphology 2012, 179, 300–314. https://doi.org/10.1016/j.geomorph.2012.08.021.

Supplementary material to the paper: Jarzyna A., Bąbel M., Ługowski D., Vladi F. 2022. Morphology of dome- and tepee-like landforms generated by expansive hydration of weathering anhydrite: a case study at Dingwall, Nova Scotia, Canada. In: Geomorphology in the Digital Era. A. Muzirafuti, G. Randazzo, S. Lanza (Eds.), Special Issue of Applied Sciences.

Figure S2

Hydration landforms on the orthophotomap and digital surface models with their extent, documentary number, azimuth of the elongation, entrance to the cavity, the heighest and the lowest elevation points and direction of maximum lateral expansion (the north direction in legend concerns all the maps).

Legend

1 — extent of the hydration form and its number

Az — azimuth of the elongation

direction of maximum lateral expansion

entrance to the cavity or cave

184 — the highest and the lowest point within hydration form*

entrance line to the cavity

N

* - for selected forms documented with the model 3D or 2.5D (terrestrial photogrammetry) elevation points [m a.s.l.] were determined on the basis of these models

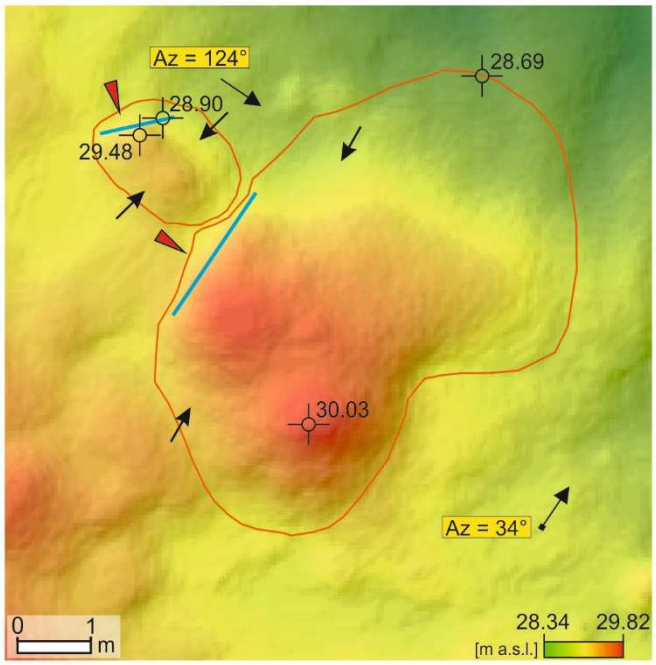

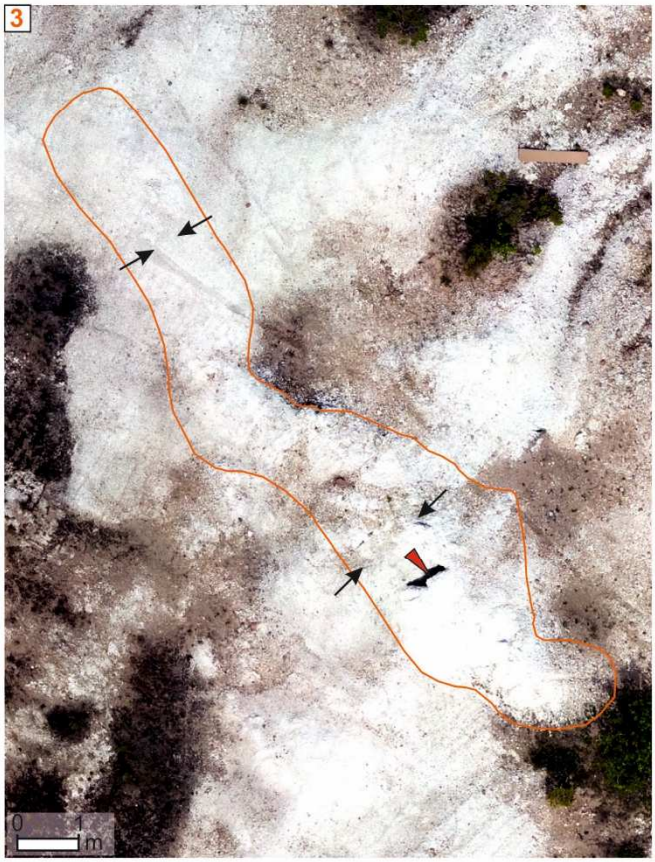

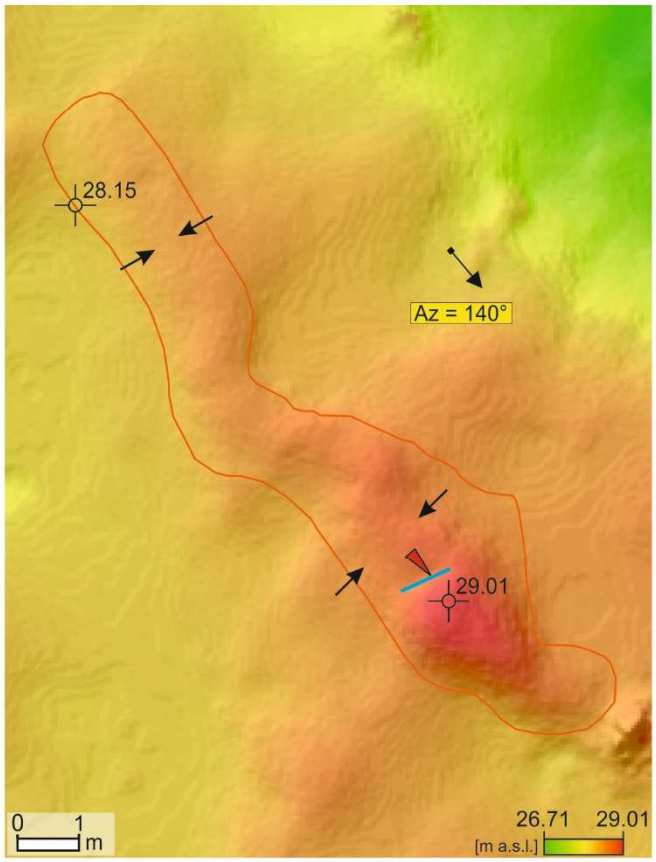

Supplementary material to the paper: Jarzyna A., Bąbel M., Ługowski D., Vladi F. 2022. Morphology of dome- and tepee-like landforms generated by expansive hydration of weathering anhydrite: a case study at Dingwall, Nova Scotia, Canada. In: Geomorphology in the Digital Era. A. Muzirafuti, G. Randazzo, S. Lanza (Eds.), Special Issue of Applied Sciences.

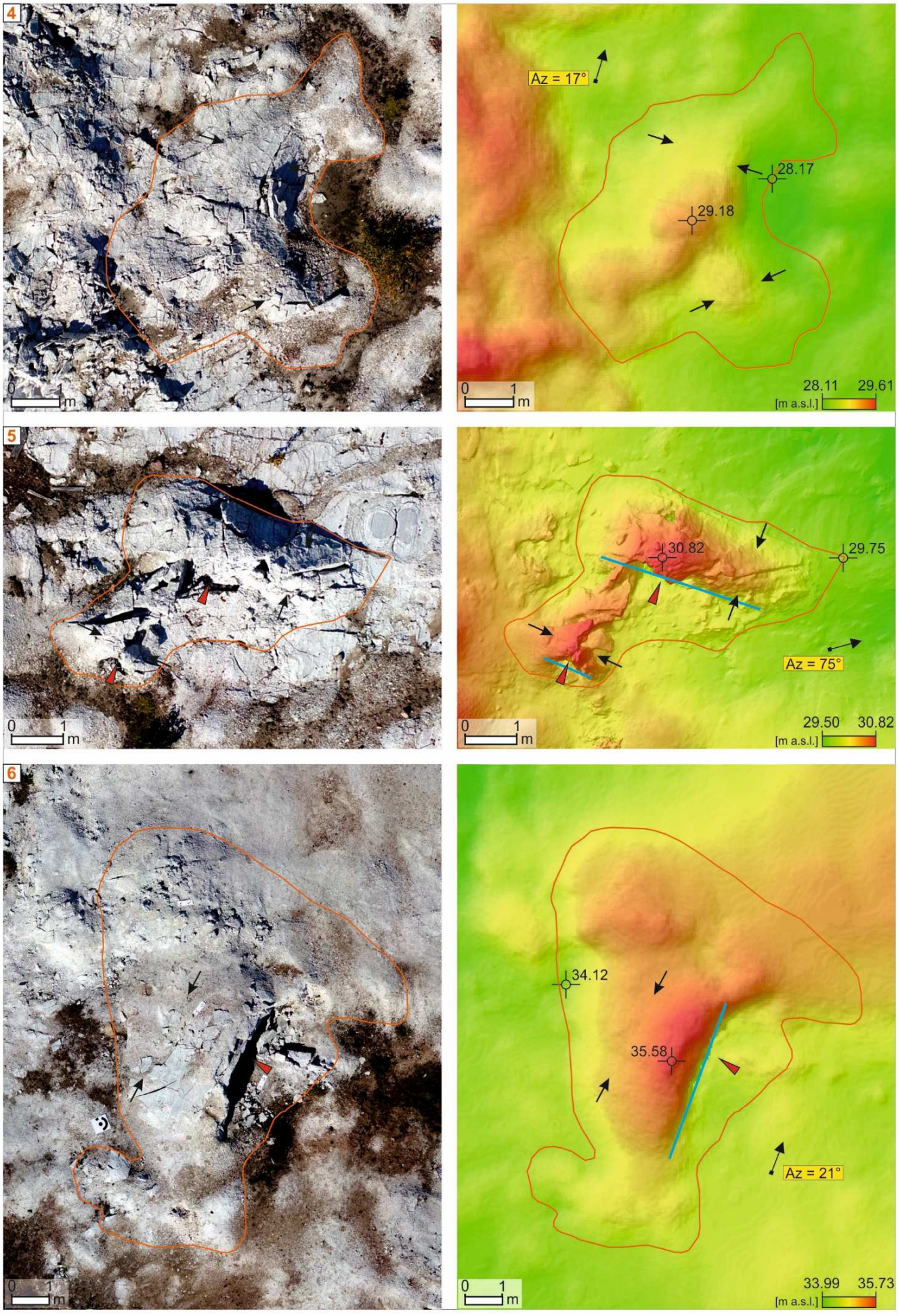

Supplementary material to the paper: Jarzyna A., Bąbel M., Ługowski D., Vladi F. 2022. Morphology of dome- and tepee-like landforms generated by expansive hydration of weathering anhydrite: a case study at Dingwall, Nova Scotia, Canada. In: Geomorphology in the Digital Era. A. Muzirafuti, G. Randazzo, S. Lanza (Eds.), Special Issue of Applied Sciences.

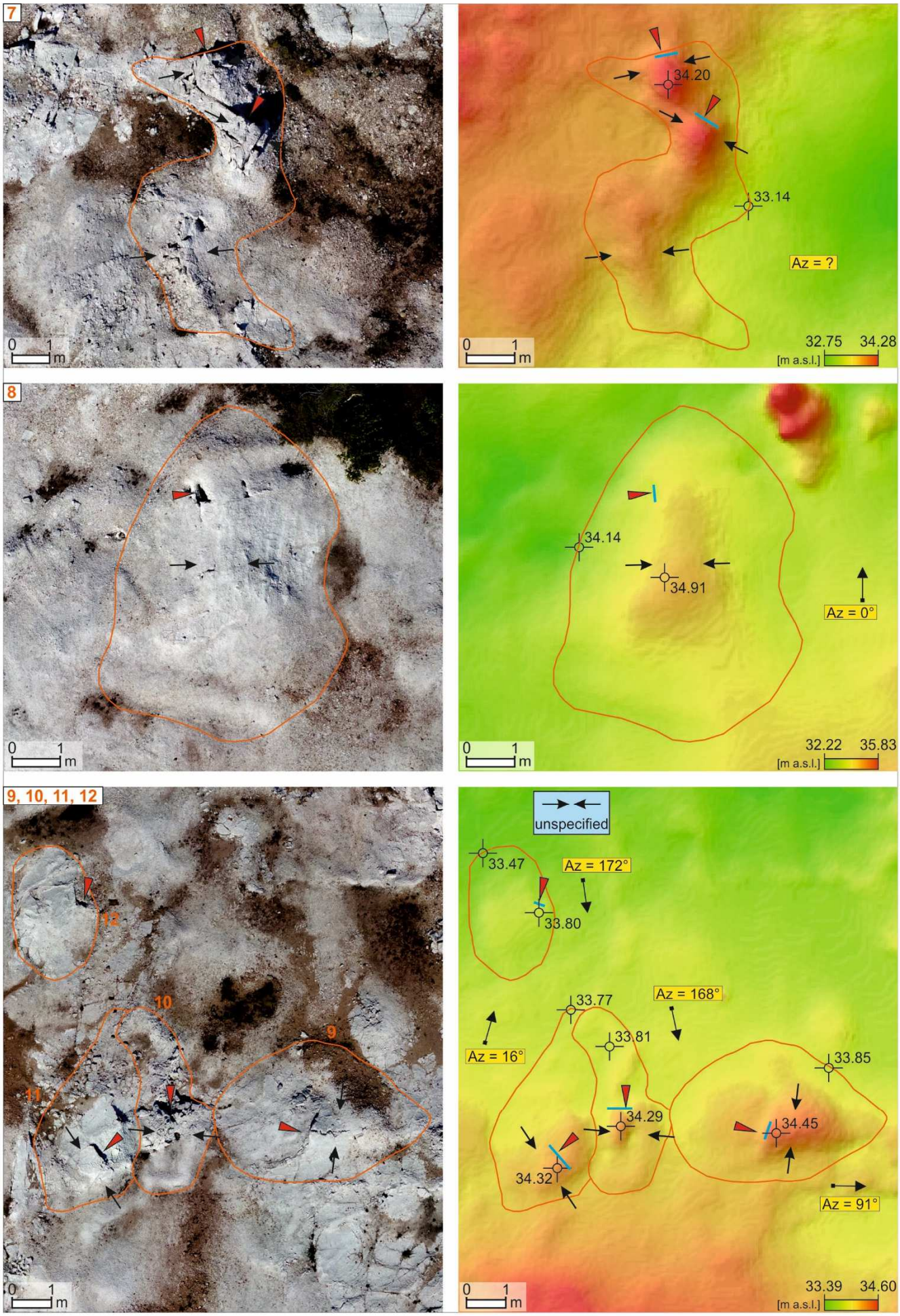

Supplementary material to the paper: Jarzyna A., Bąbel M., Ługowski D., Vladi F. 2022. Morphology of dome- and tepee-like landforms generated by expansive hydration of weathering anhydrite: a case study at Dingwall, Nova Scotia, Canada. In: Geomorphology in the Digital Era. A. Muzirafuti, G. Randazzo, S. Lanza (Eds.), Special Issue of Applied Sciences.

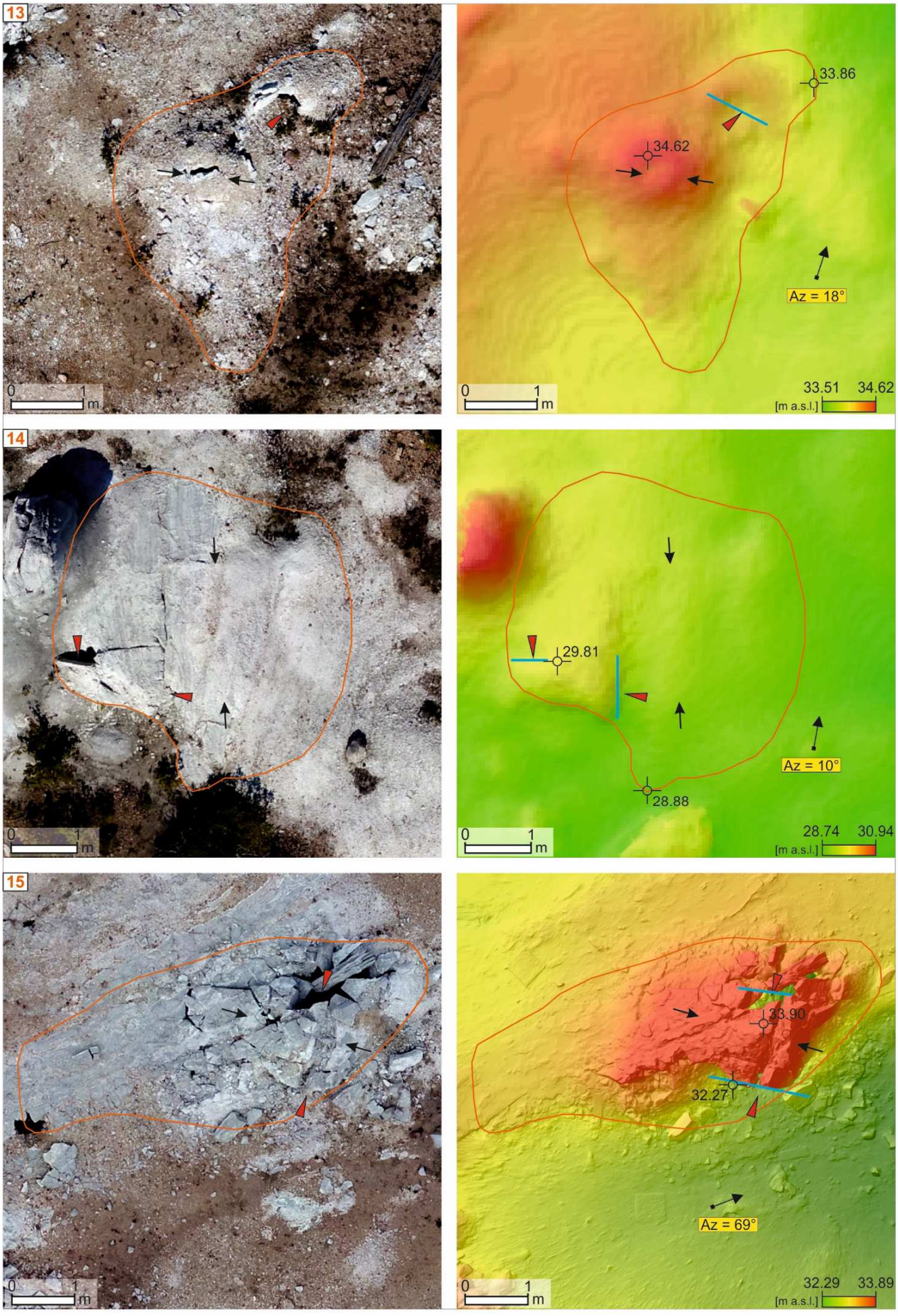

Supplementary material to the paper: Jarzyna A., Bąbel M., Ługowski D., Vladi F. 2022. Morphology of dome- and tepee-like landforms generated by expansive hydration of weathering anhydrite: a case study at Dingwall, Nova Scotia, Canada. In: Geomorphology in the Digital Era. A. Muzirafuti, G. Randazzo, S. Lanza (Eds.), Special Issue of Applied Sciences.

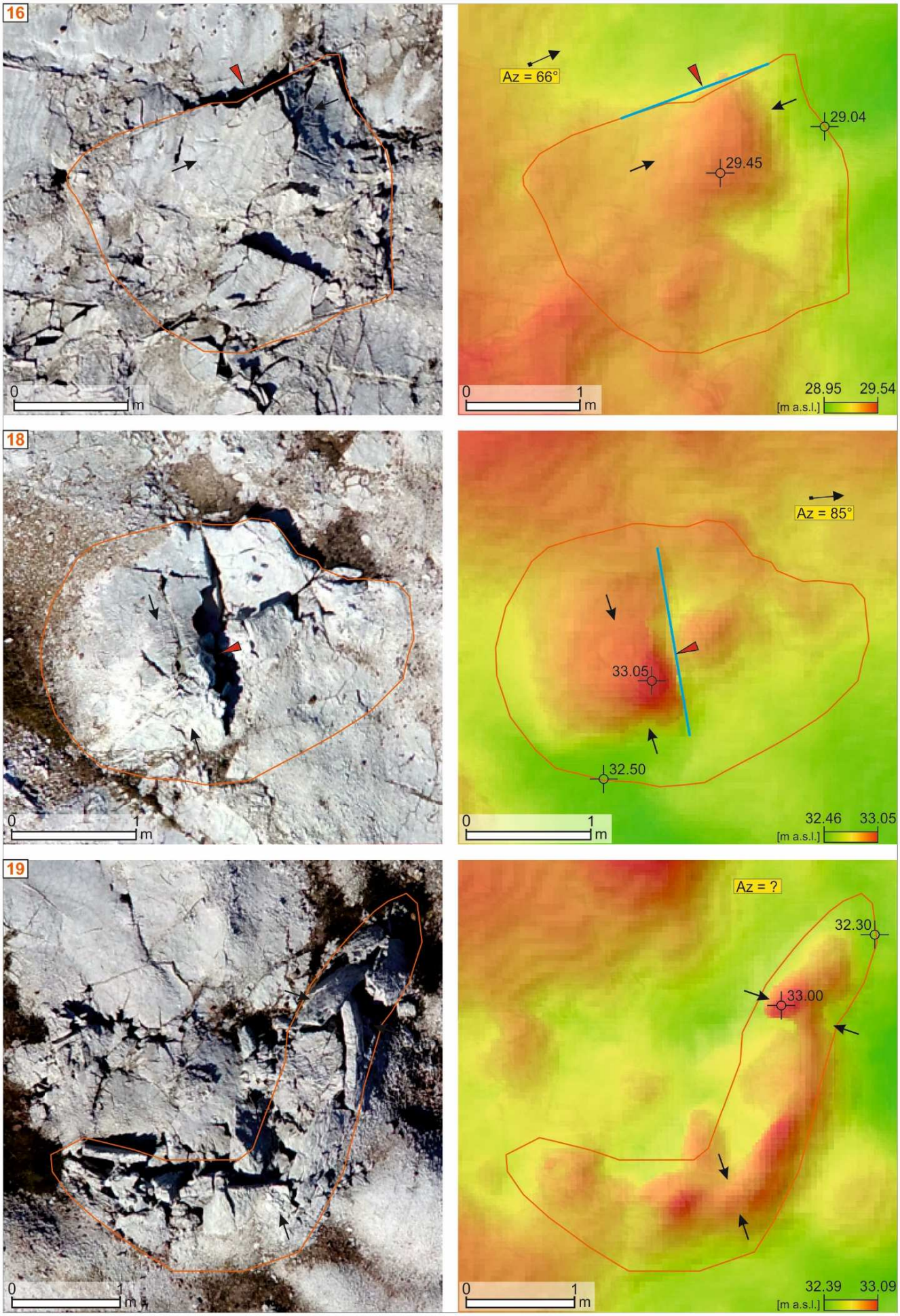

Supplementary material to the paper: Jarzyna A., Bąbel M., Ługowski D., Vladi F. 2022. Morphology of dome- and tepee-like landforms generated by expansive hydration of weathering anhydrite: a case study at Dingwall, Nova Scotia, Canada. In: Geomorphology in the Digital Era. A. Muzirafuti, G. Randazzo, S. Lanza (Eds.), Special Issue of Applied Sciences.

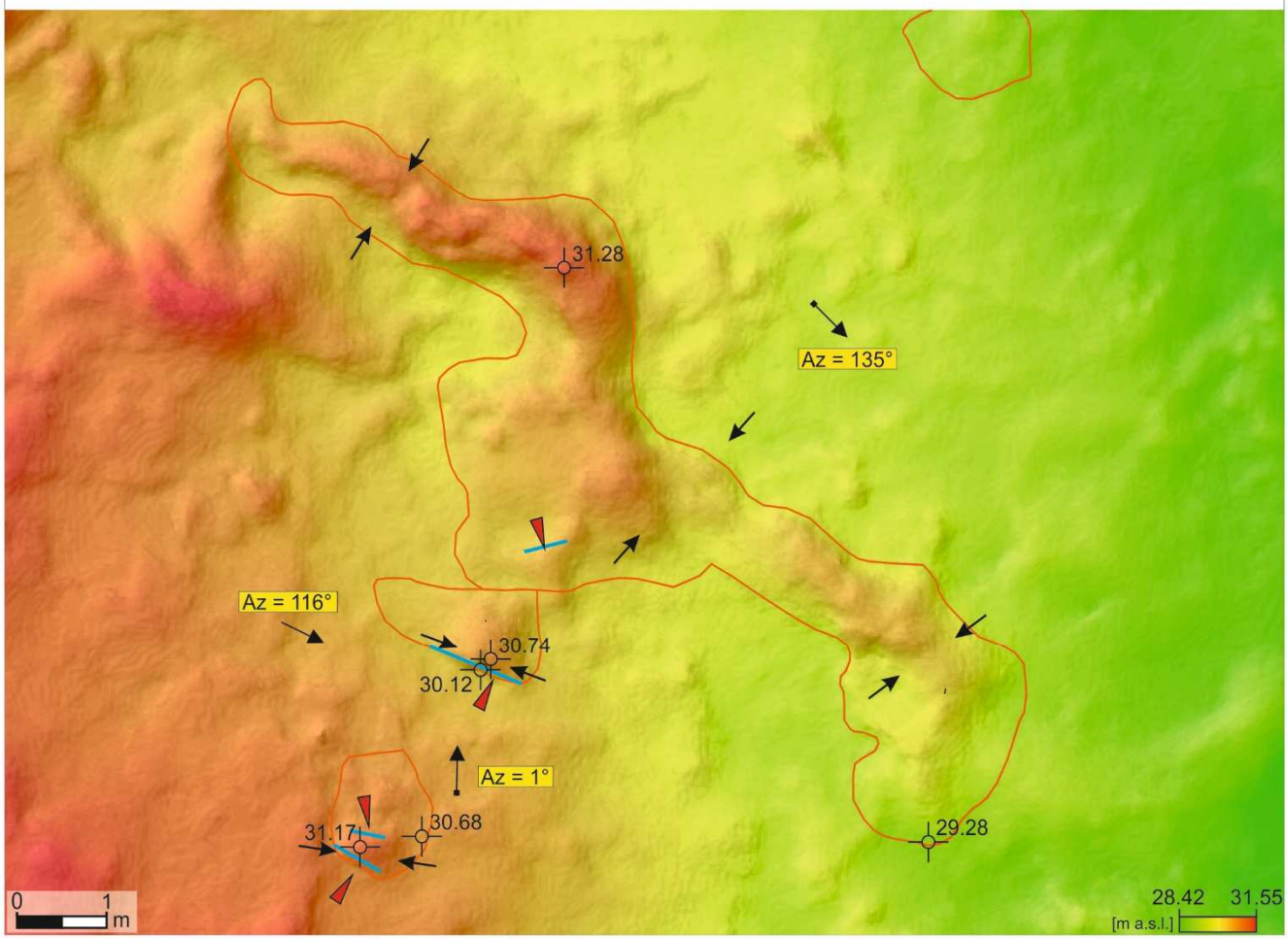

Supplementary material to the paper: Jarzyna A., Bąbel M., Ługowski D., Vladi F. 2022. Morphology of dome- and tepee-like landforms generated by expansive hydration of weathering anhydrite: a case study at Dingwall, Nova Scotia, Canada. In: Geomorphology in the Digital Era. A. Muzirafuti, G. Randazzo, S. Lanza (Eds.), Special Issue of Applied Sciences.

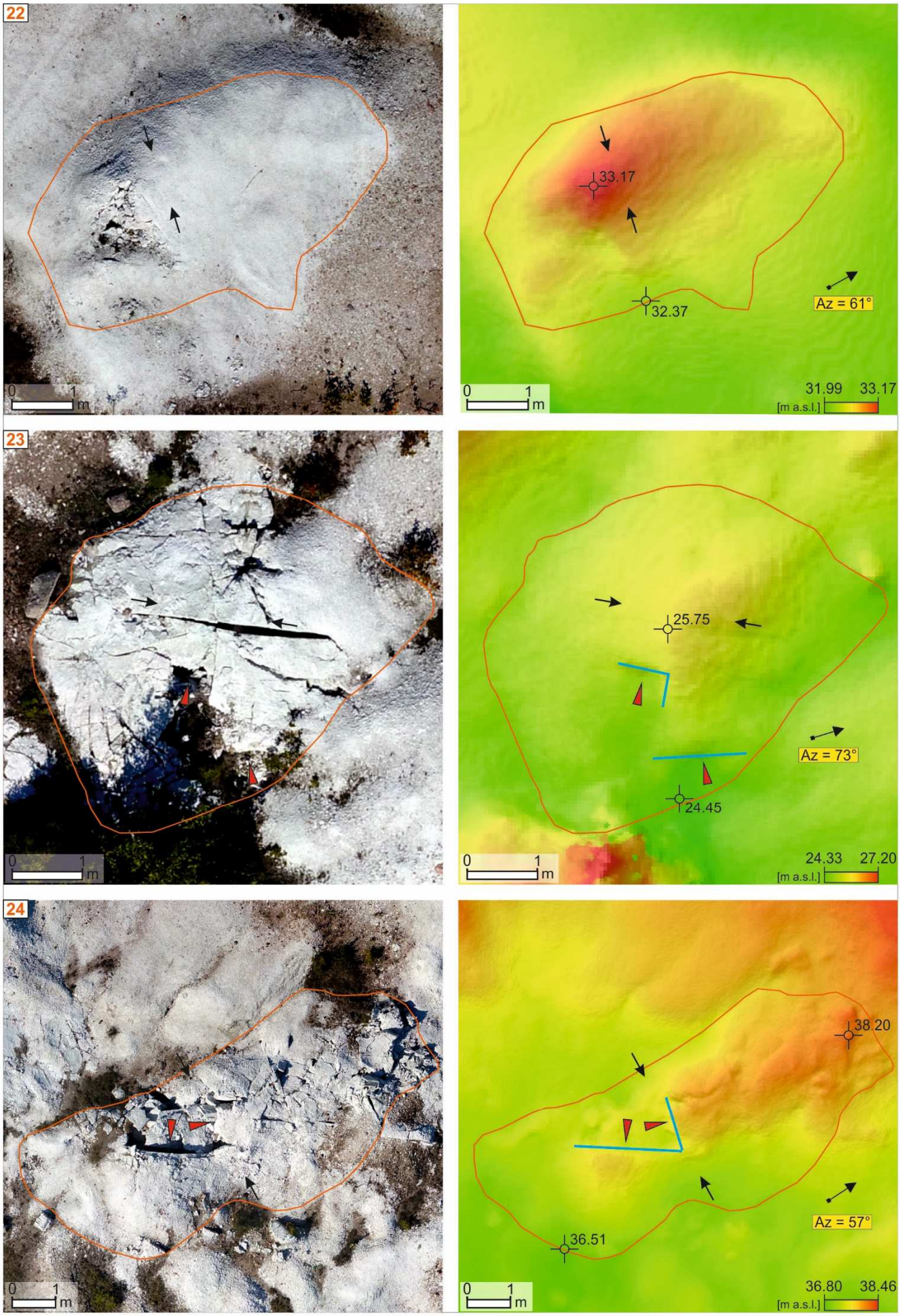

Supplementary material to the paper: Jarzyna A., Bąbel M., Ługowski D., Vladi F. 2022. Morphology of dome- and tepee-like landforms generated by expansive hydration of weathering anhydrite: a case study at Dingwall, Nova Scotia, Canada. In: Geomorphology in the Digital Era. A. Muzirafuti, G. Randazzo, S. Lanza (Eds.), Special Issue of Applied Sciences.

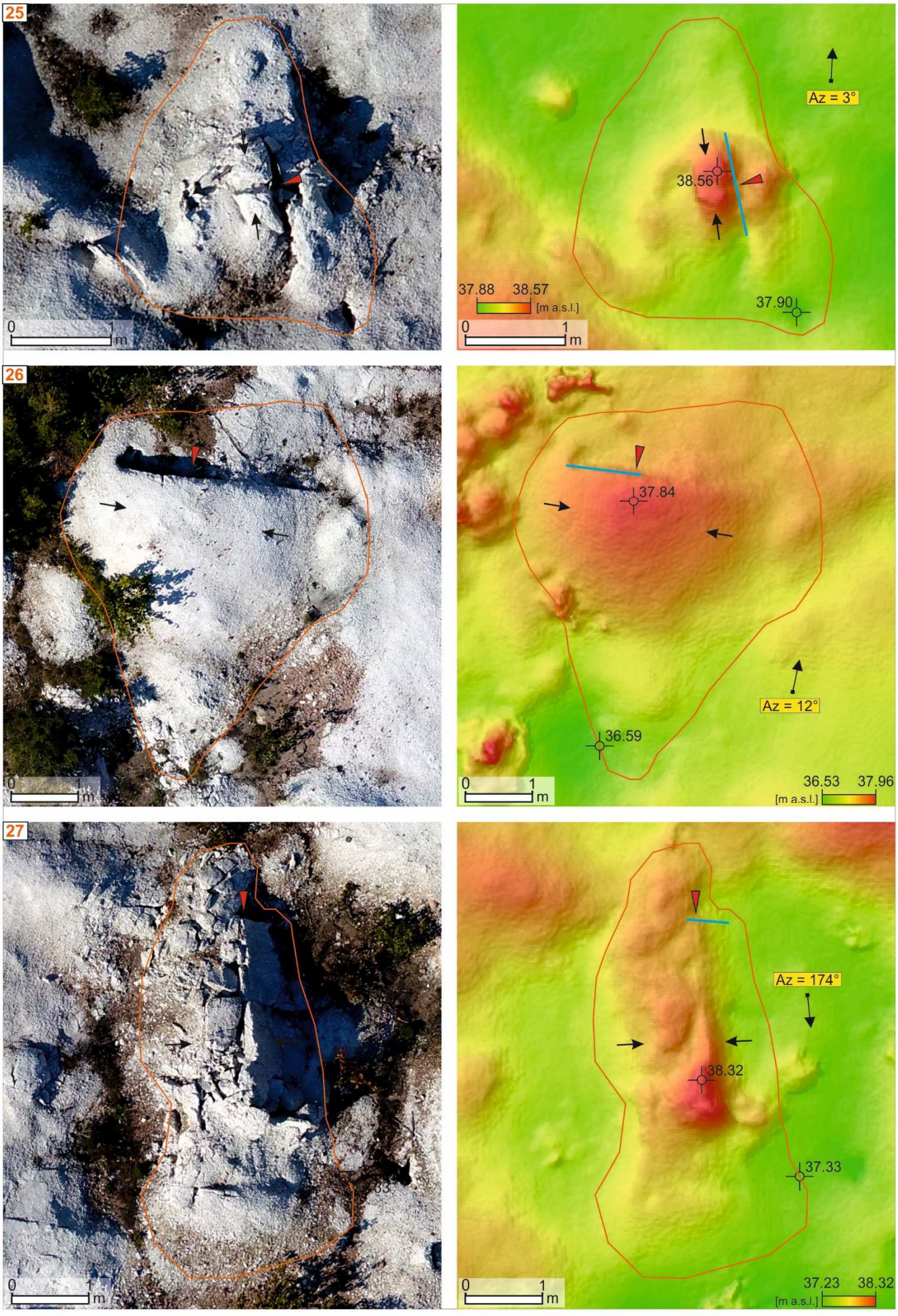

Supplementary material to the paper: Jarzyna A., Bąbel M., Ługowski D., Vladi F. 2022. Morphology of dome- and tepee-like landforms generated by expansive hydration of weathering anhydrite: a case study at Dingwall, Nova Scotia, Canada. In: Geomorphology in the Digital Era. A. Muzirafuti, G. Randazzo, S. Lanza (Eds.), Special Issue of Applied Sciences.

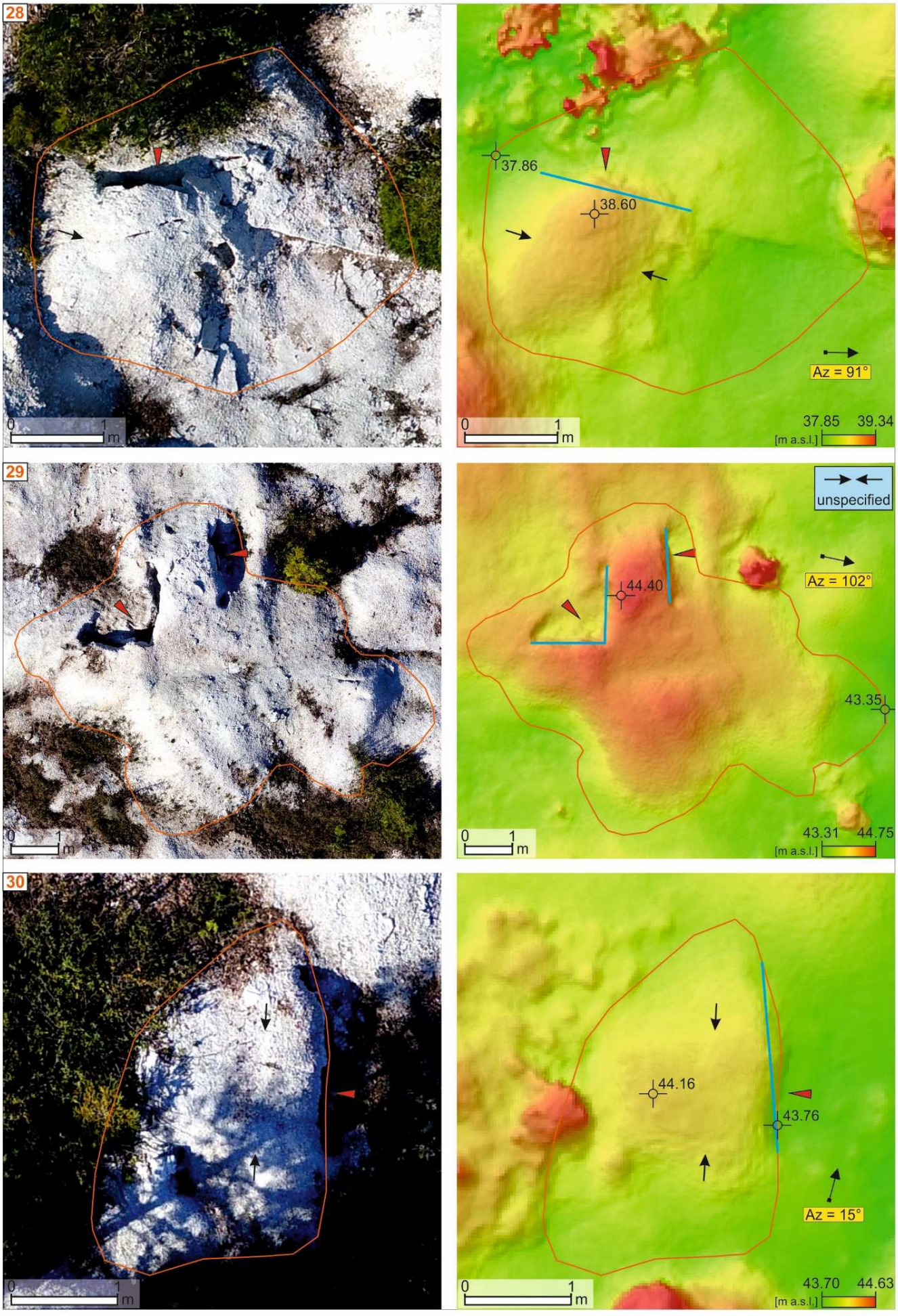

Supplementary material to the paper: Jarzyna A., Bąbel M., Ługowski D., Vladi F. 2022. Morphology of dome- and tepee-like landforms generated by expansive hydration of weathering anhydrite: a case study at Dingwall, Nova Scotia, Canada. In: Geomorphology in the Digital Era. A. Muzirafuti, G. Randazzo, S. Lanza (Eds.), Special Issue of Applied Sciences.

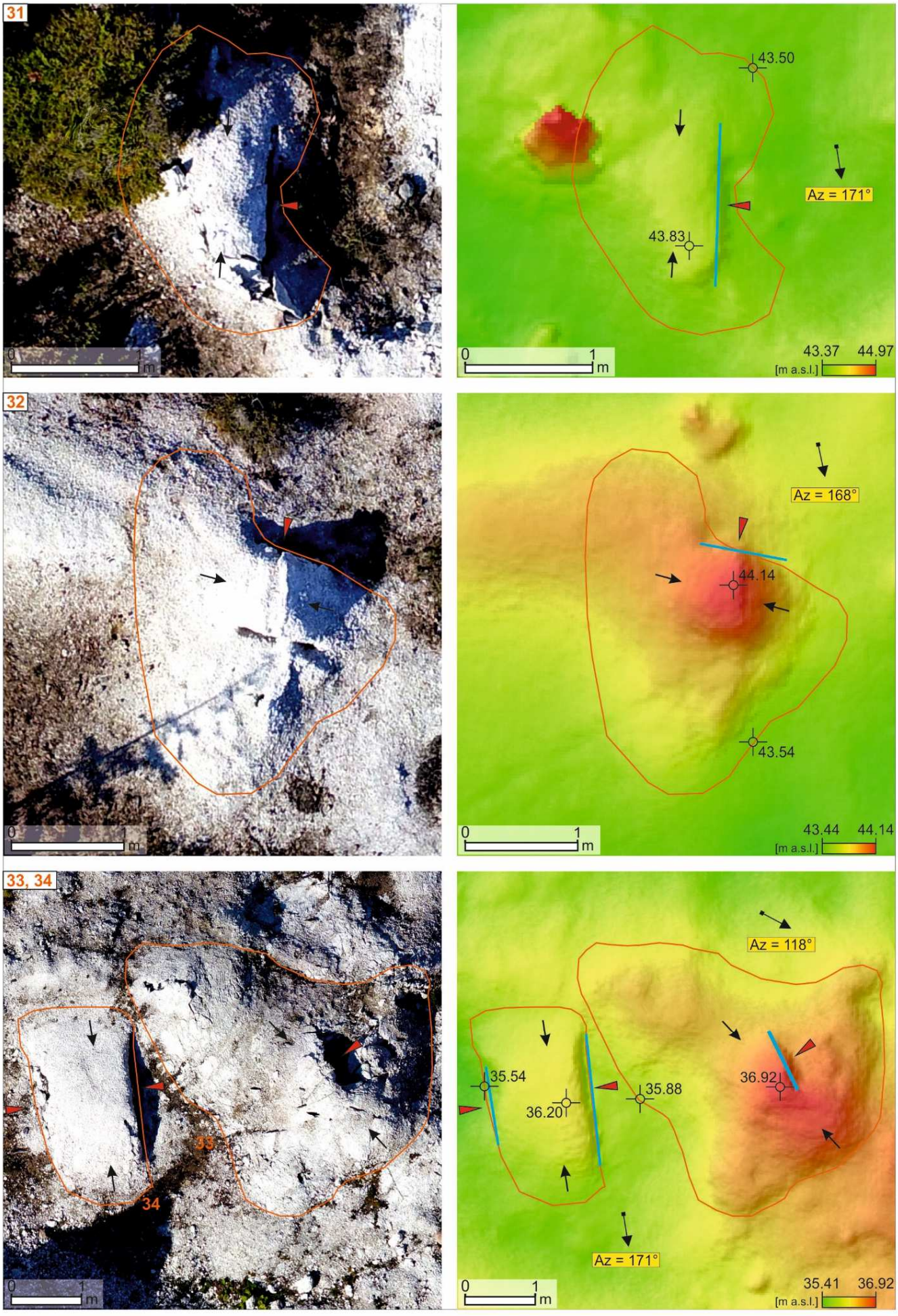

Supplementary material to the paper: Jarzyna A., Bąbel M., Ługowski D., Vladi F. 2022. Morphology of dome- and tepee-like landforms generated by expansive hydration of weathering anhydrite: a case study at Dingwall, Nova Scotia, Canada. In: Geomorphology in the Digital Era. A. Muzirafuti, G. Randazzo, S. Lanza (Eds.), Special Issue of Applied Sciences.

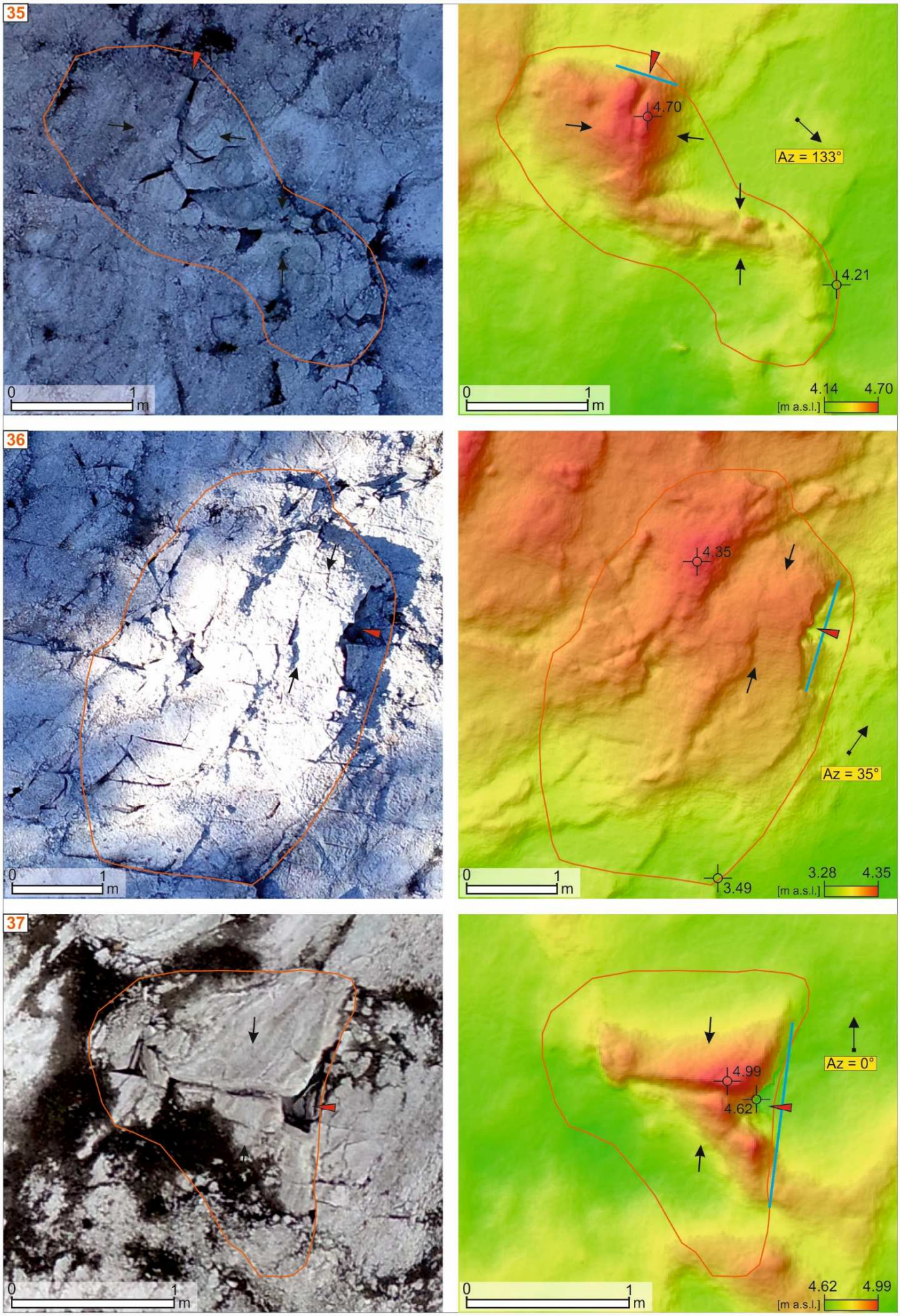

Supplementary material to the paper: Jarzyna A., Bąbel M., Ługowski D., Vladi F. 2022. Morphology of dome- and tepee-like landforms generated by expansive hydration of weathering anhydrite: a case study at Dingwall, Nova Scotia, Canada. In: Geomorphology in the Digital Era. A. Muzirafuti, G. Randazzo, S. Lanza (Eds.), Special Issue of Applied Sciences.

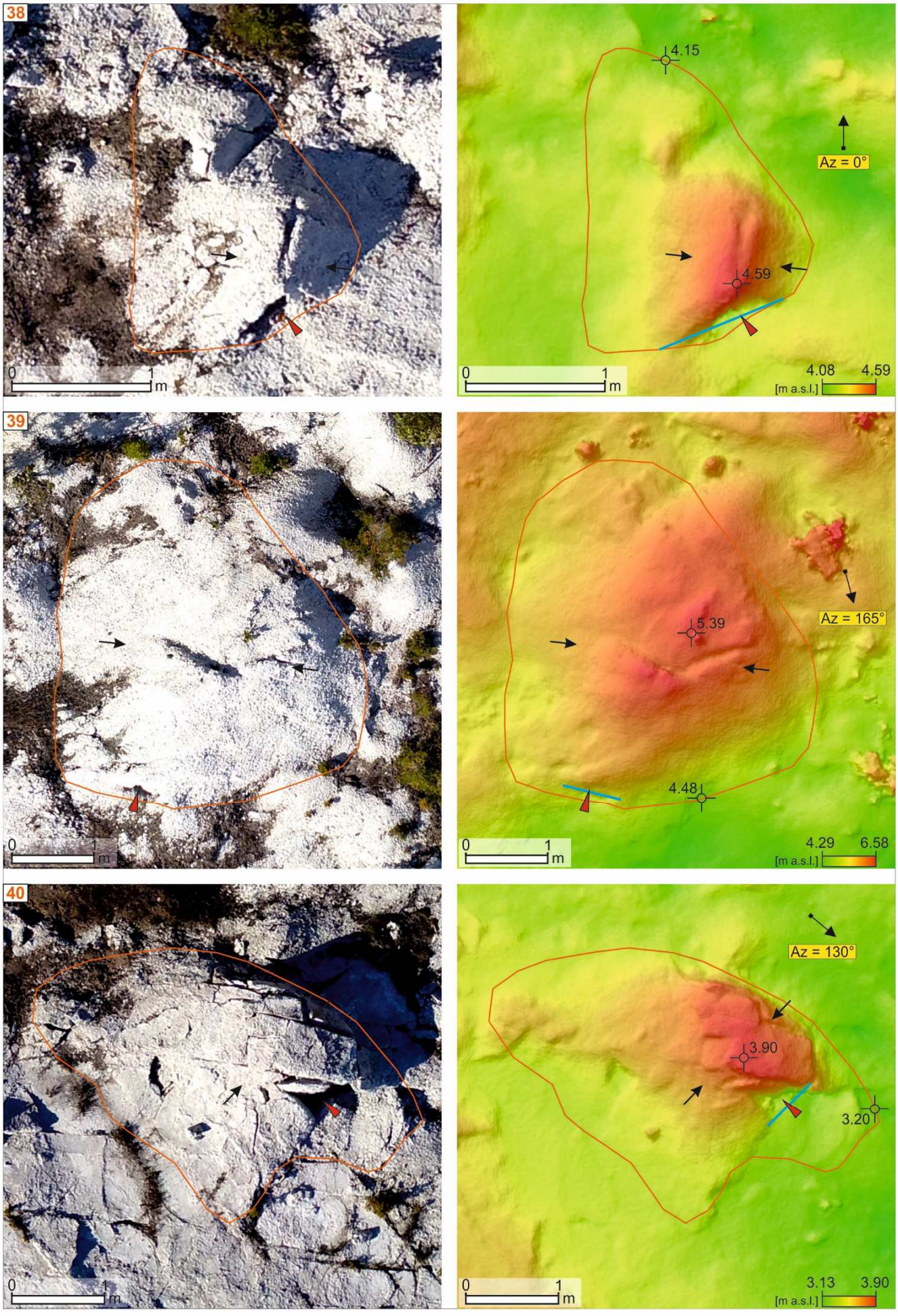

Supplementary material to the paper: Jarzyna A., Bąbel M., Ługowski D., Vladi F. 2022. Morphology of dome- and tepee-like landforms generated by expansive hydration of weathering anhydrite: a case study at Dingwall, Nova Scotia, Canada. In: Geomorphology in the Digital Era. A. Muzirafuti, G. Randazzo, S. Lanza (Eds.), Special Issue of Applied Sciences.

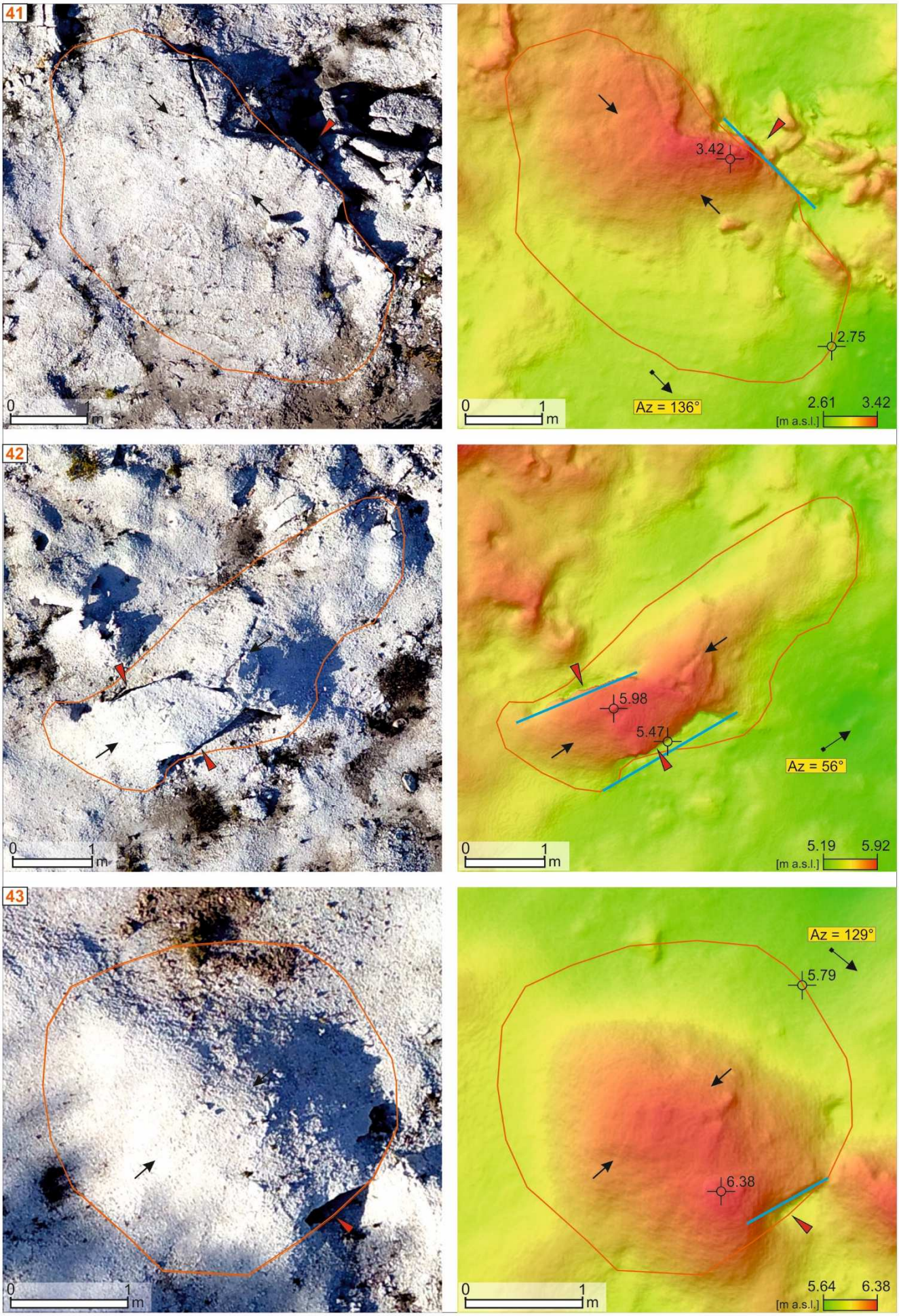

Supplementary material to the paper: Jarzyna A., Bąbel M., Ługowski D., Vladi F. 2022. Morphology of dome- and tepee-like landforms generated by expansive hydration of weathering anhydrite: a case study at Dingwall, Nova Scotia, Canada. In: Geomorphology in the Digital Era. A. Muzirafuti, G. Randazzo, S. Lanza (Eds.), Special Issue of Applied Sciences.

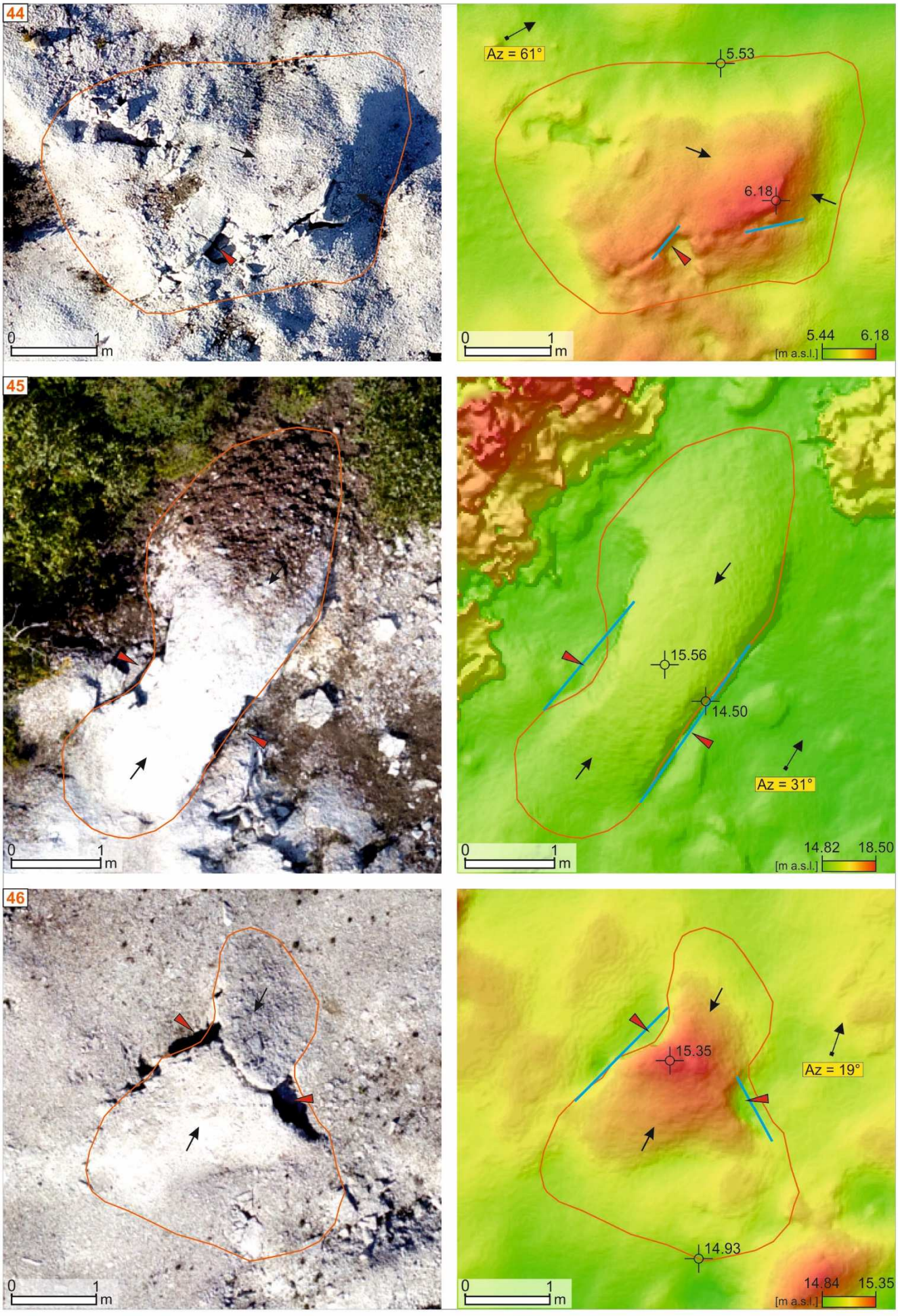

Supplementary material to the paper: Jarzyna A., Bąbel M., Ługowski D., Vladi F. 2022. Morphology of dome- and tepee-like landforms generated by expansive hydration of weathering anhydrite: a case study at Dingwall, Nova Scotia, Canada. In: Geomorphology in the Digital Era. A. Muzirafuti, G. Randazzo, S. Lanza (Eds.), Special Issue of Applied Sciences.

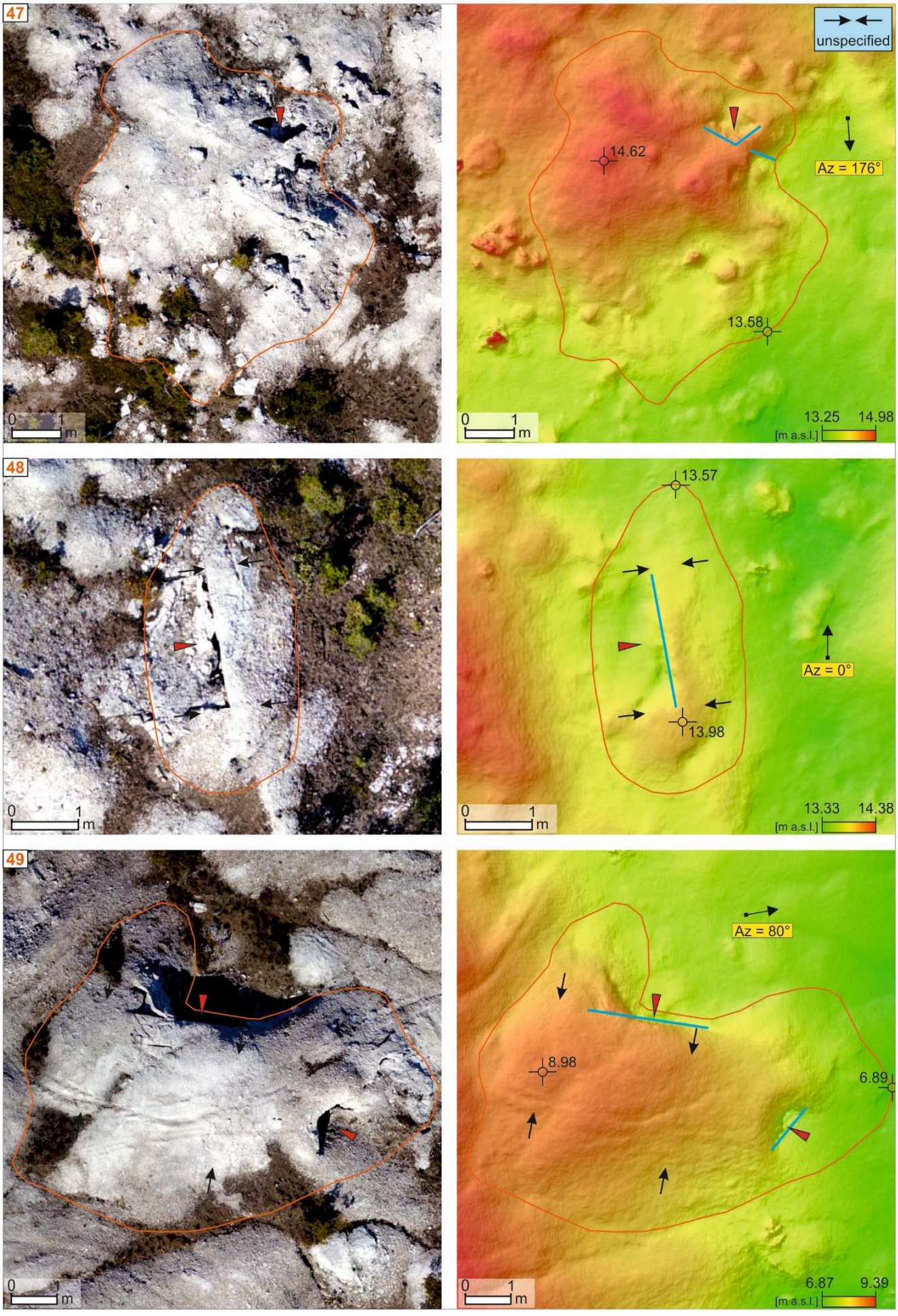

Supplementary material to the paper: Jarzyna A., Bąbel M., Ługowski D., Vladi F. 2022. Morphology of dome- and tepee-like landforms generated by expansive hydration of weathering anhydrite: a case study at Dingwall, Nova Scotia, Canada. In: Geomorphology in the Digital Era. A. Muzirafuti, G. Randazzo, S. Lanza (Eds.), Special Issue of Applied Sciences.

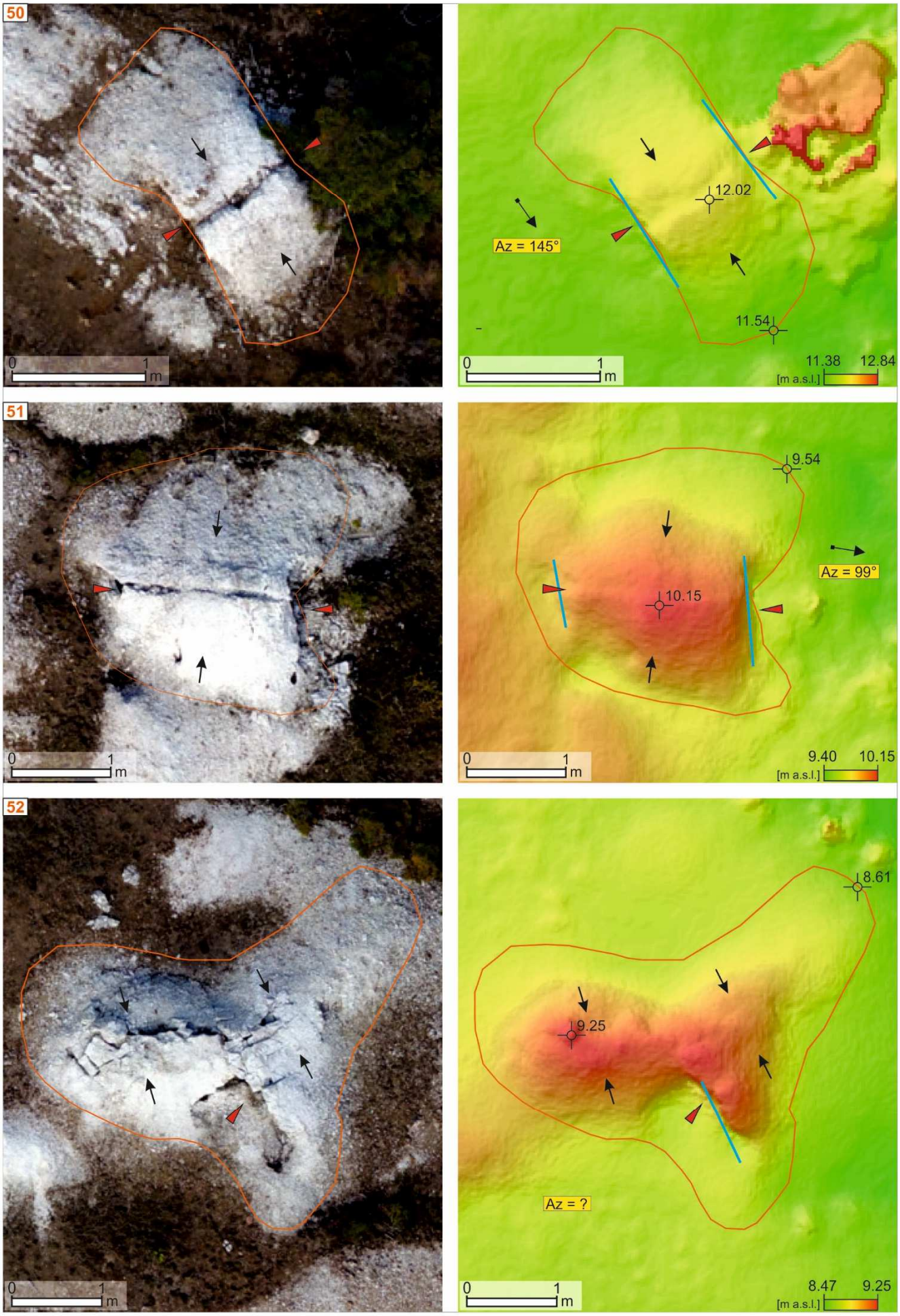

Supplementary material to the paper: Jarzyna A., Bąbel M., Ługowski D., Vladi F. 2022. Morphology of dome- and tepee-like landforms generated by expansive hydration of weathering anhydrite: a case study at Dingwall, Nova Scotia, Canada. In: Geomorphology in the Digital Era. A. Muzirafuti, G. Randazzo, S. Lanza (Eds.), Special Issue of Applied Sciences.

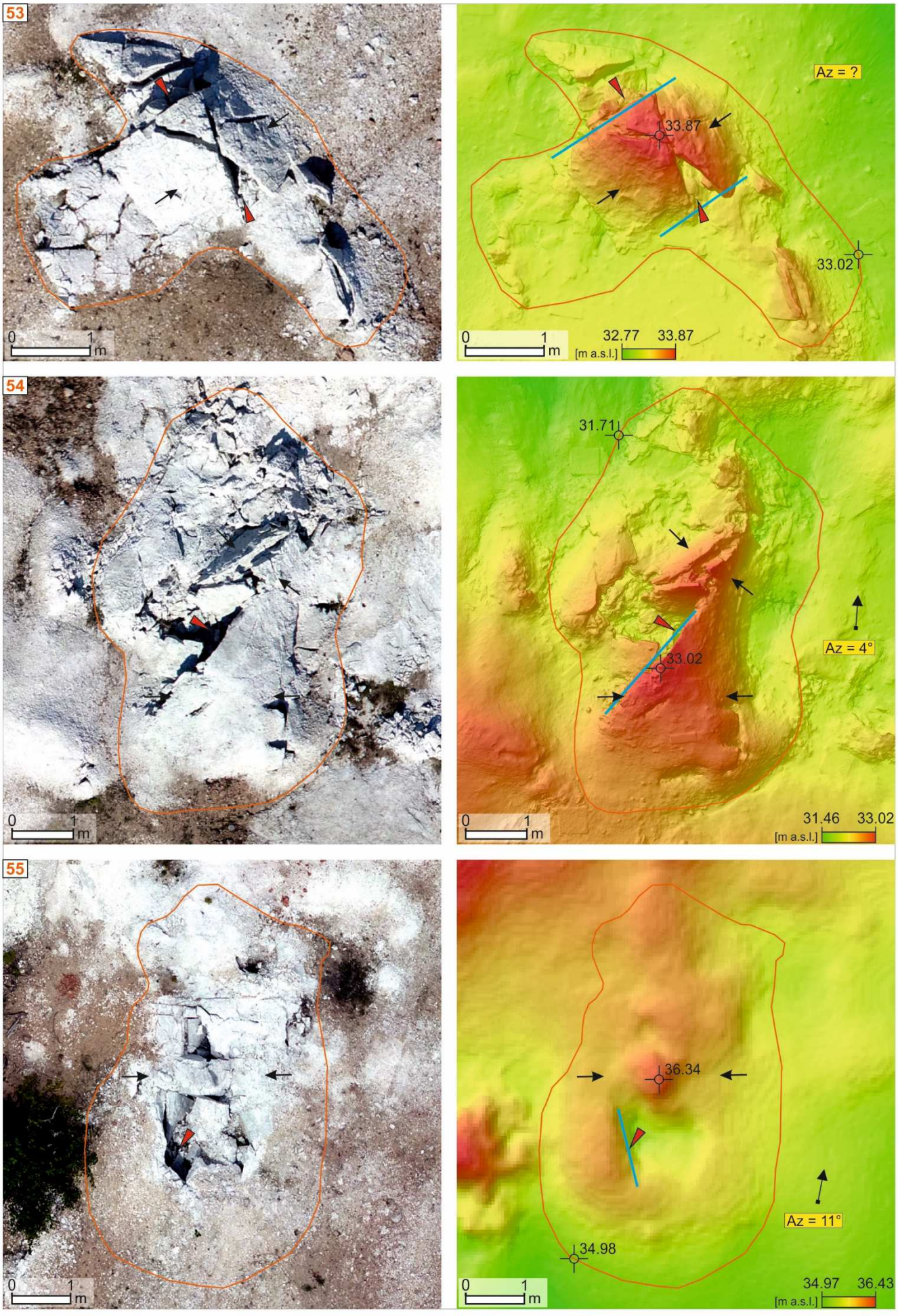

Supplementary material to the paper: Jarzyna A., Bąbel M., Ługowski D., Vladi F. 2022. Morphology of dome- and tepee-like landforms generated by expansive hydration of weathering anhydrite: a case study at Dingwall, Nova Scotia, Canada. In: Geomorphology in the Digital Era. A. Muzirafuti, G. Randazzo, S. Lanza (Eds.), Special Issue of Applied Sciences.

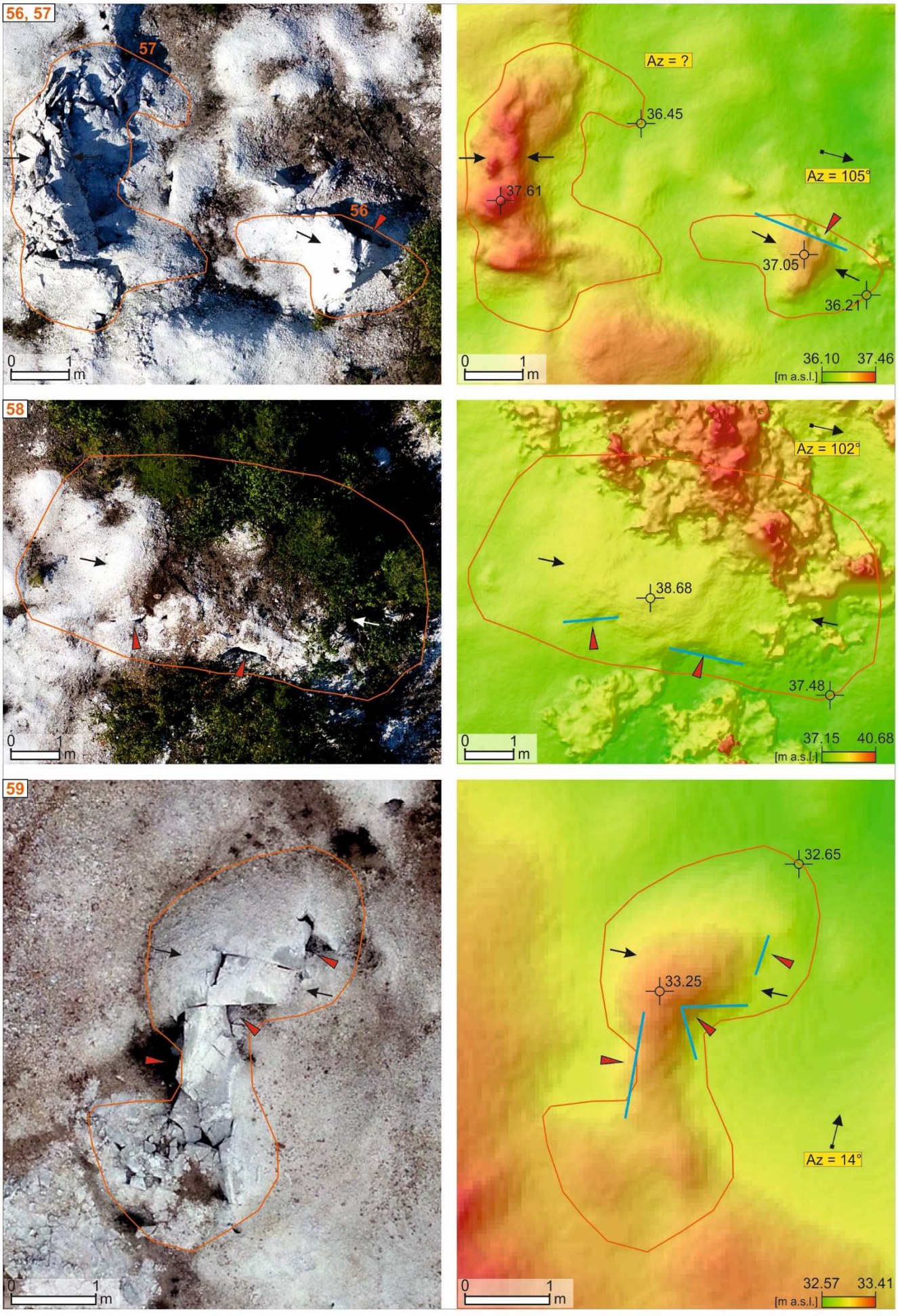

Supplementary material to the paper: Jarzyna A., Bąbel M., Ługowski D., Vladi F. 2022. Morphology of dome- and tepee-like landforms generated by expansive hydration of weathering anhydrite: a case study at Dingwall, Nova Scotia, Canada. In: Geomorphology in the Digital Era. A. Muzirafuti, G. Randazzo, S. Lanza (Eds.), Special Issue of Applied Sciences.

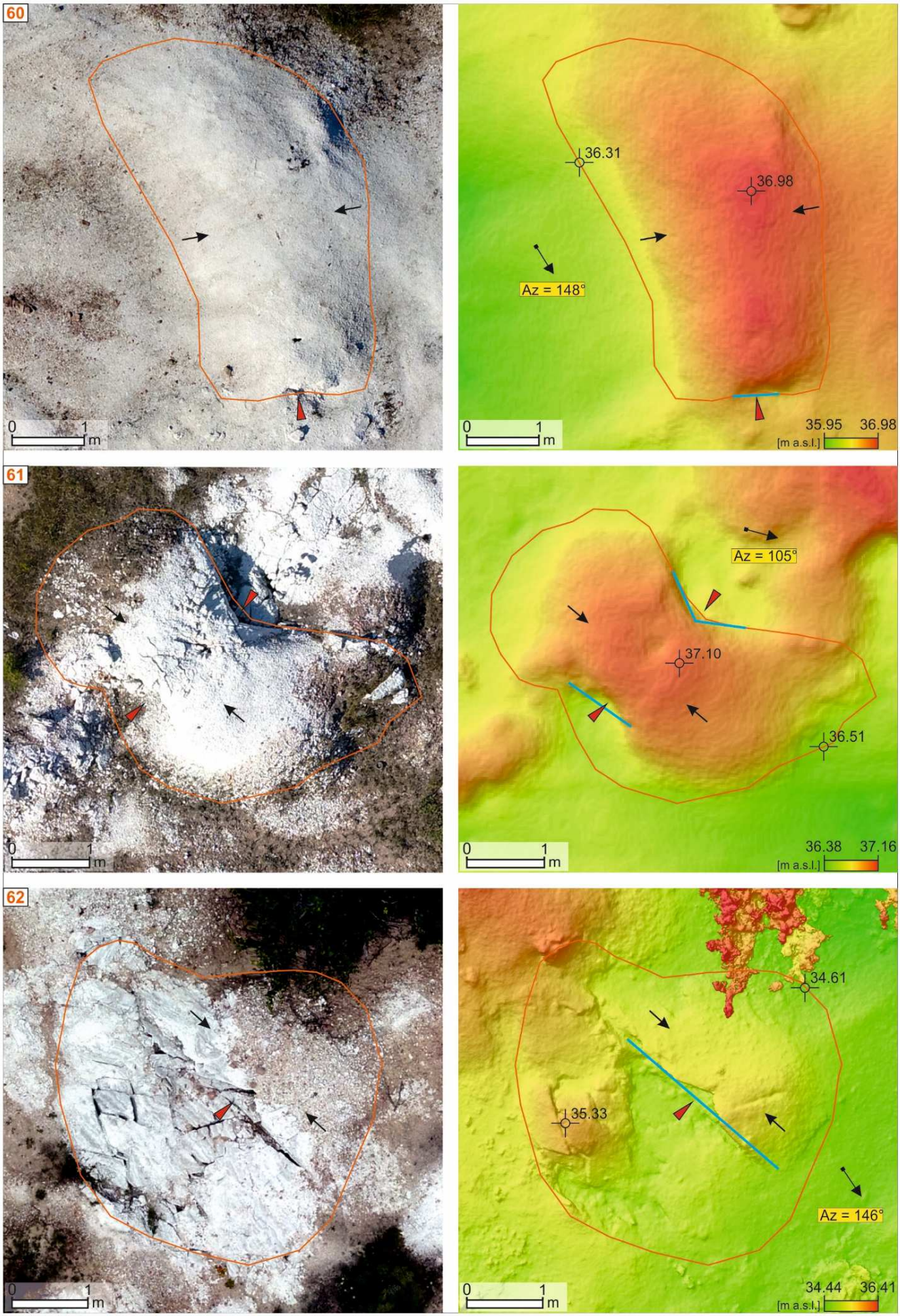

Supplementary material to the paper: Jarzyna A., Bąbel M., Ługowski D., Vladi F. 2022. Morphology of dome- and tepee-like landforms generated by expansive hydration of weathering anhydrite: a case study at Dingwall, Nova Scotia, Canada. In: Geomorphology in the Digital Era. A. Muzirafuti, G. Randazzo, S. Lanza (Eds.), Special Issue of Applied Sciences.

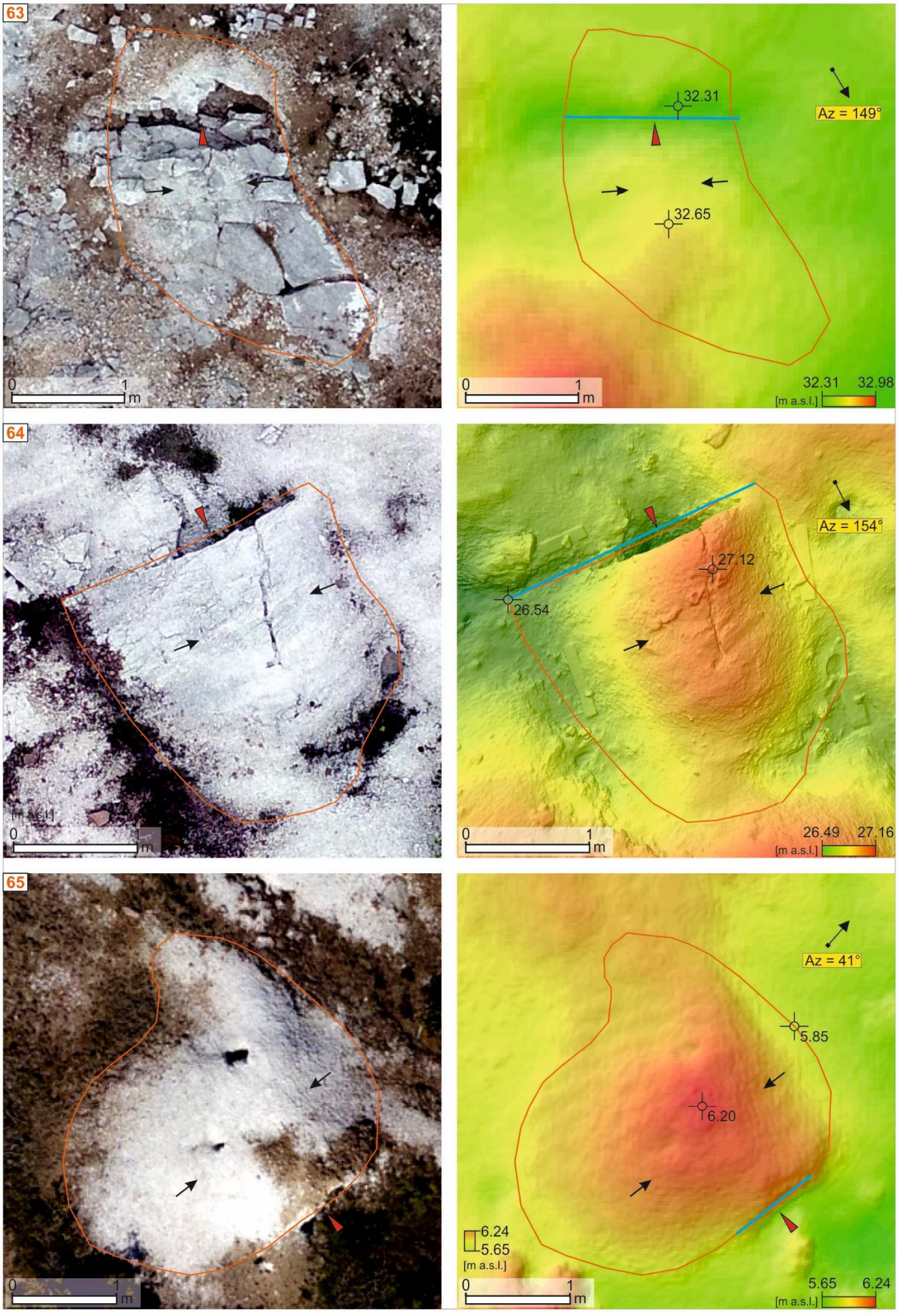

Supplementary material to the paper: Jarzyna A., Bąbel M., Ługowski D., Vladi F. 2022. Morphology of dome- and tepee-like landforms generated by expansive hydration of weathering anhydrite: a case study at Dingwall, Nova Scotia, Canada. In: Geomorphology in the Digital Era. A. Muzirafuti, G. Randazzo, S. Lanza (Eds.), Special Issue of Applied Sciences.

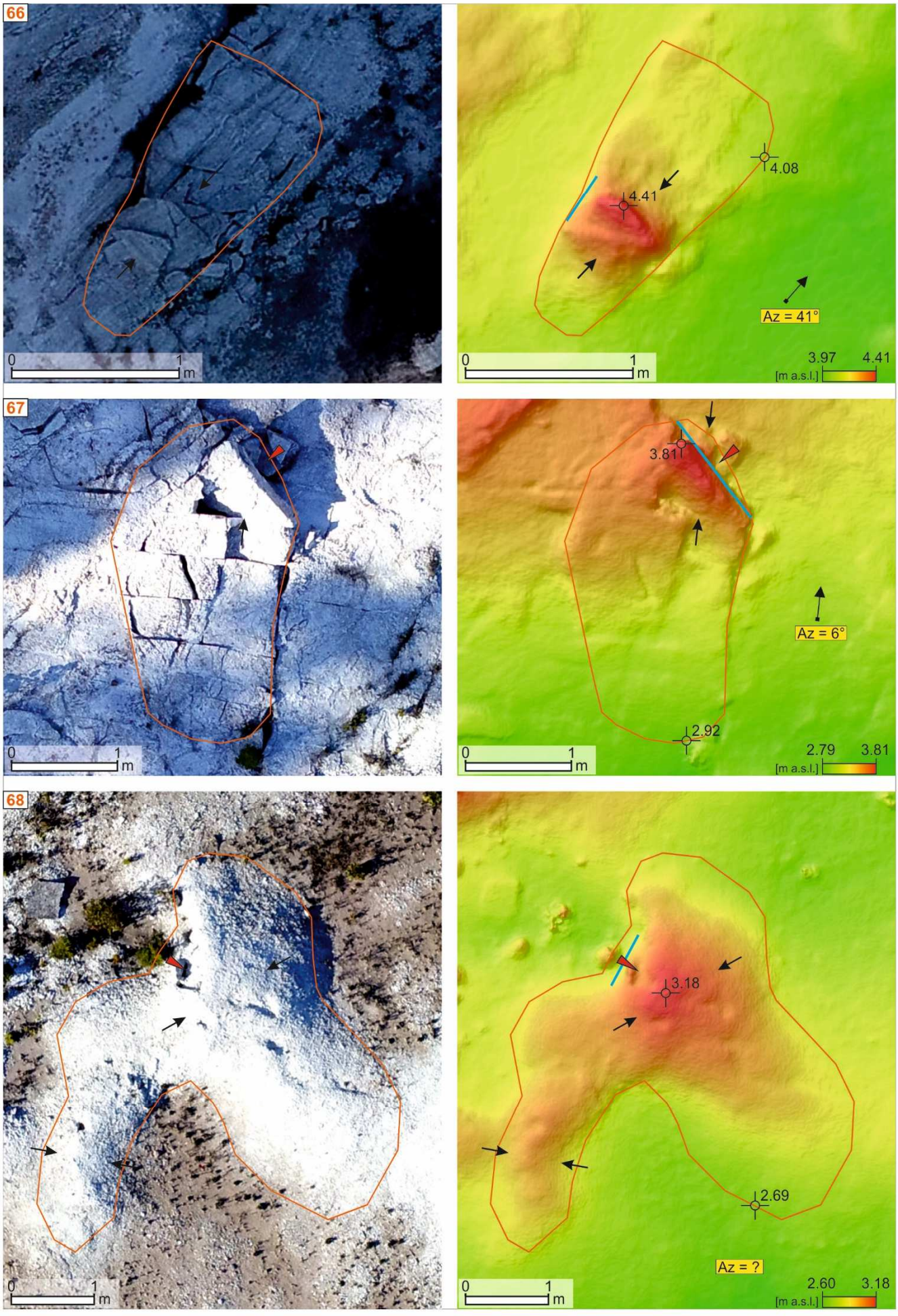

Supplementary material to the paper: Jarzyna A., Bąbel M., Ługowski D., Vladi F. 2022. Morphology of dome- and tepee-like landforms generated by expansive hydration of weathering anhydrite: a case study at Dingwall, Nova Scotia, Canada. In: Geomorphology in the Digital Era. A. Muzirafuti, G. Randazzo, S. Lanza (Eds.), Special Issue of Applied Sciences.

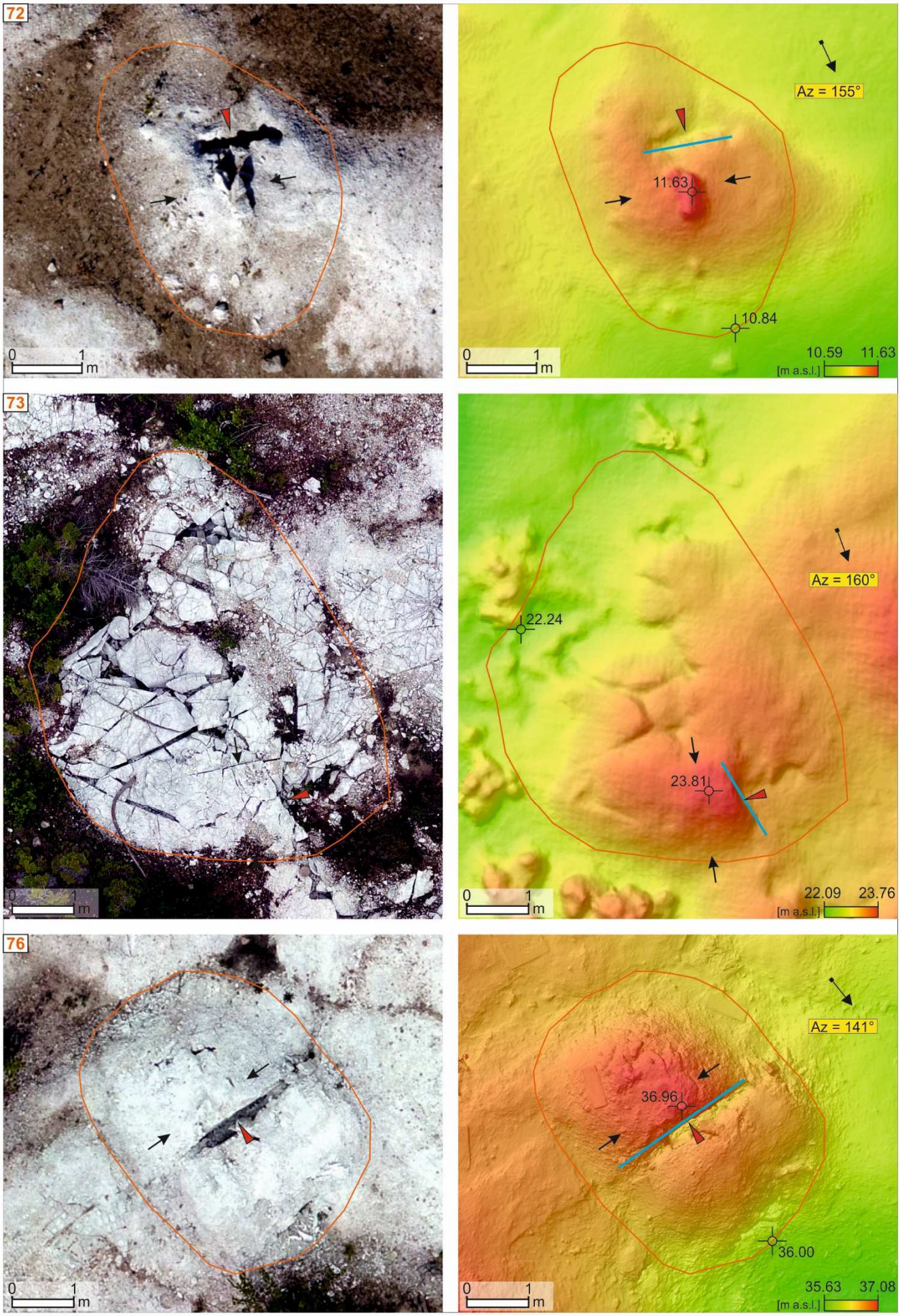

Supplementary material to the paper: Jarzyna A., Bąbel M., Ługowski D., Vladi F. 2022. Morphology of dome- and tepee-like landforms generated by expansive hydration of weathering anhydrite: a case study at Dingwall, Nova Scotia, Canada. In: Geomorphology in the Digital Era. A. Muzirafuti, G. Randazzo, S. Lanza (Eds.), Special Issue of Applied Sciences.

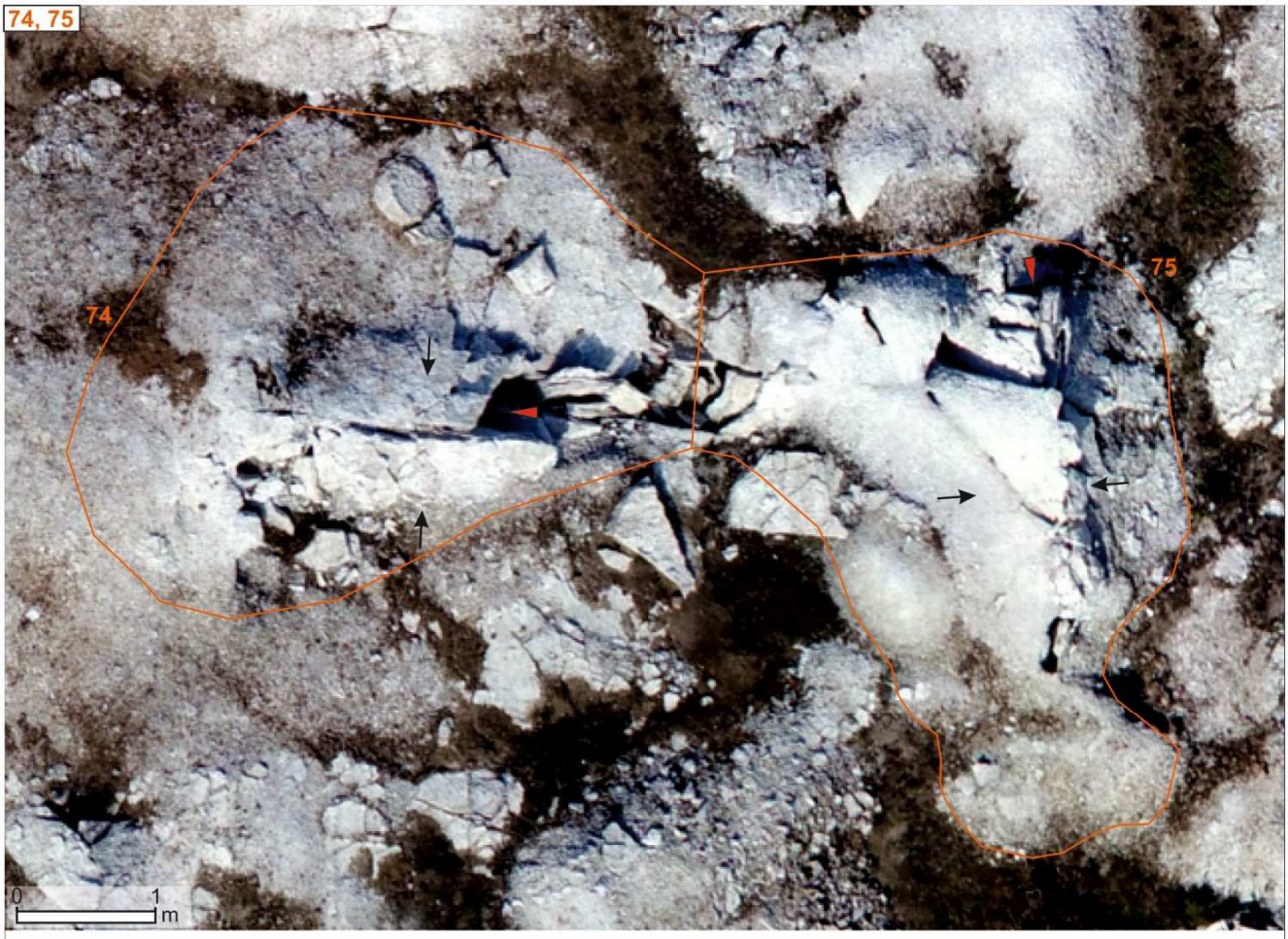

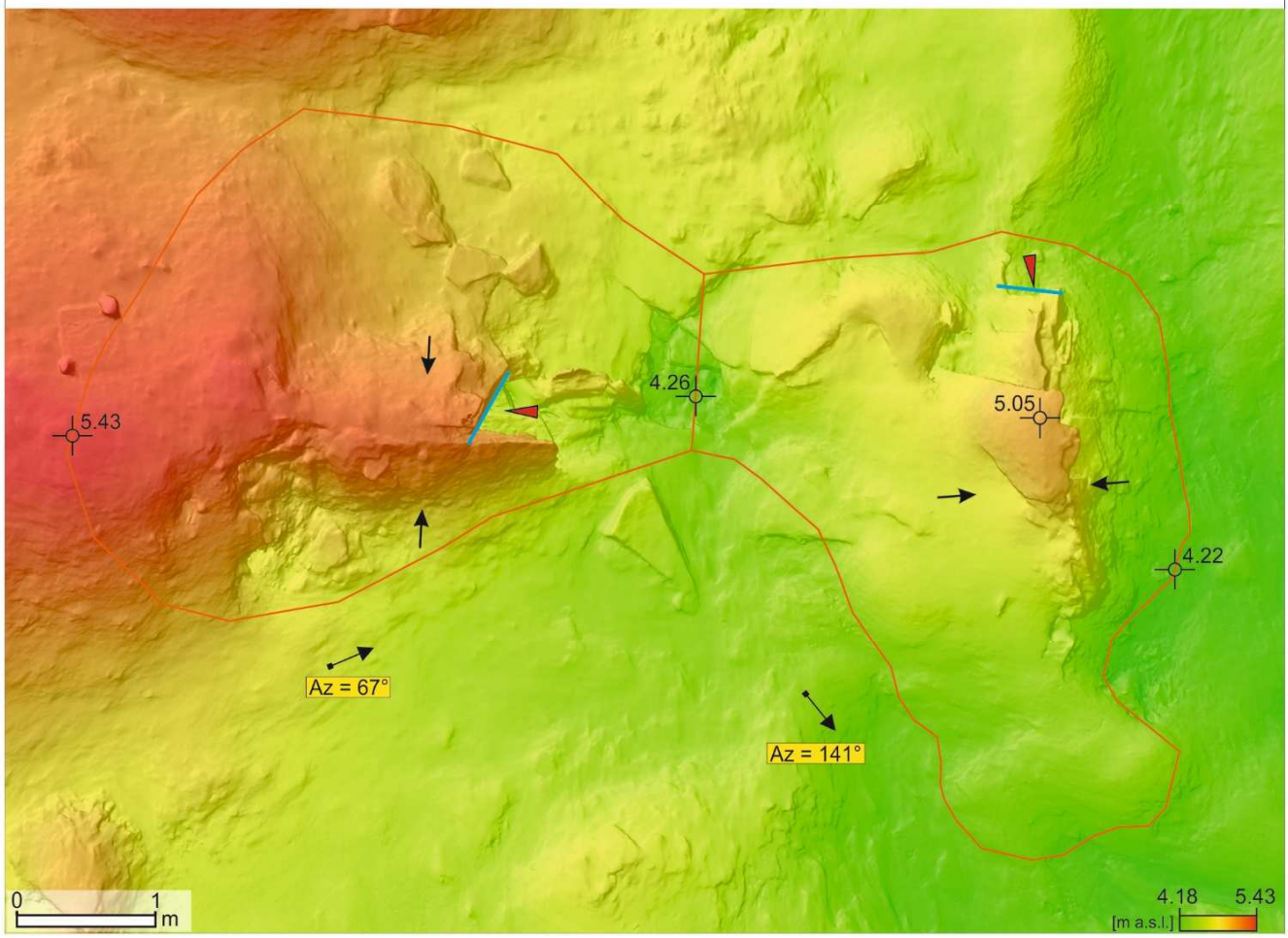

Supplementary material to the paper: Jarzyna A., Bąbel M., Ługowski D., Vladi F. 2022. Morphology of dome- and tepee-like landforms generated by expansive hydration of weathering anhydrite: a case study at Dingwall, Nova Scotia, Canada. In: Geomorphology in the Digital Era. A. Muzirafuti, G. Randazzo, S. Lanza (Eds.), Special Issue of Applied Sciences.

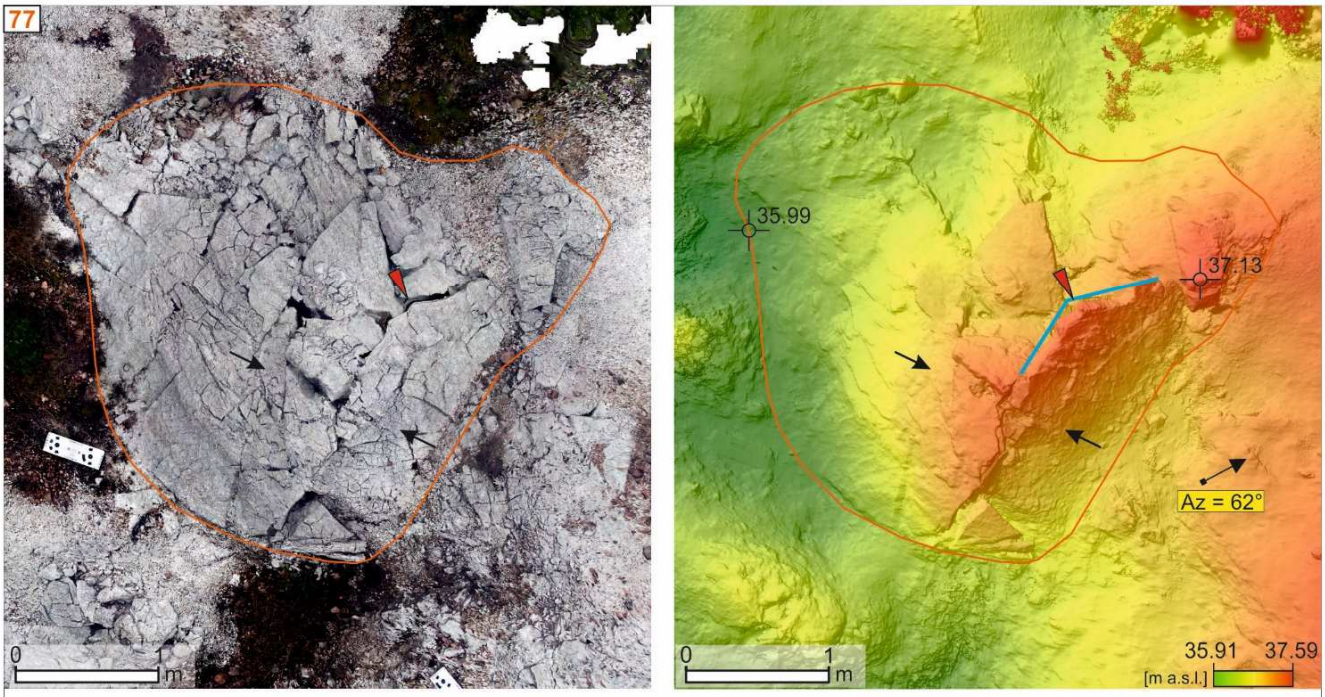

Supplementary material to the paper: Jarzyna A., Bąbel M., Ługowski D., Vladi F. 2022. Morphology of dome- and tepee-like landforms generated by expansive hydration of weathering anhydrite: a case study at Dingwall, Nova Scotia, Canada. In: Geomorphology in the Digital Era. A. Muzirafuti, G. Randazzo, S. Lanza (Eds.), Special Issue of Applied Sciences.

Figure S3

Location of hydration landforms on the basemap of satellite image (source: ArcGIS program) with characteristic of their sizes.

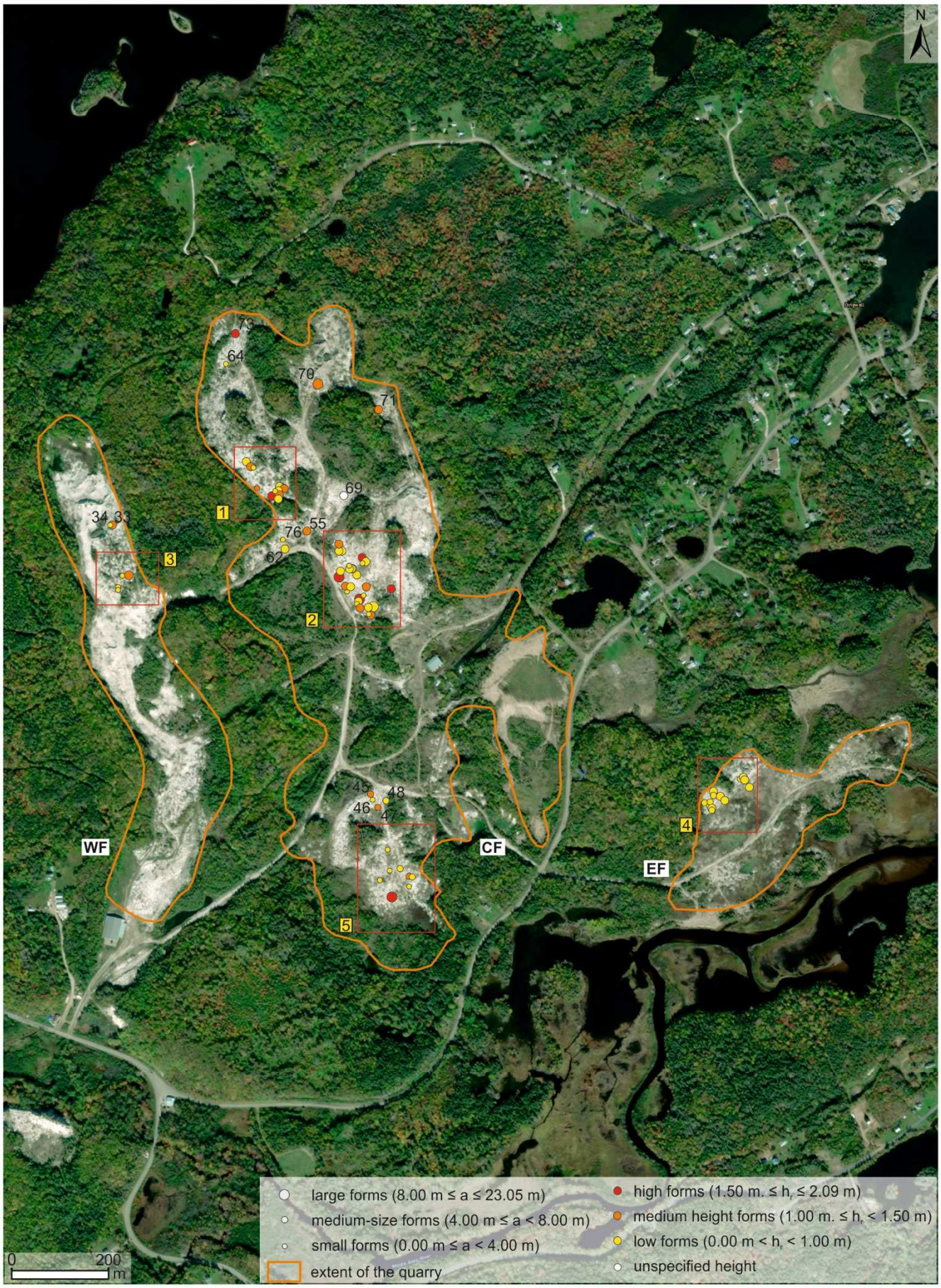

Supplementary material to the paper: Jarzyna A., Bąbel M., Ługowski D., Vladi F. 2022. Morphology of dome- and tepee-like landforms generated by expansive hydration of weathering anhydrite: a case study at Dingwall, Nova Scotia, Canada. In: Geomorphology in the Digital Era. A. Muzirafuti, G. Randazzo, S. Lanza (Eds.), Special Issue of Applied Sciences.

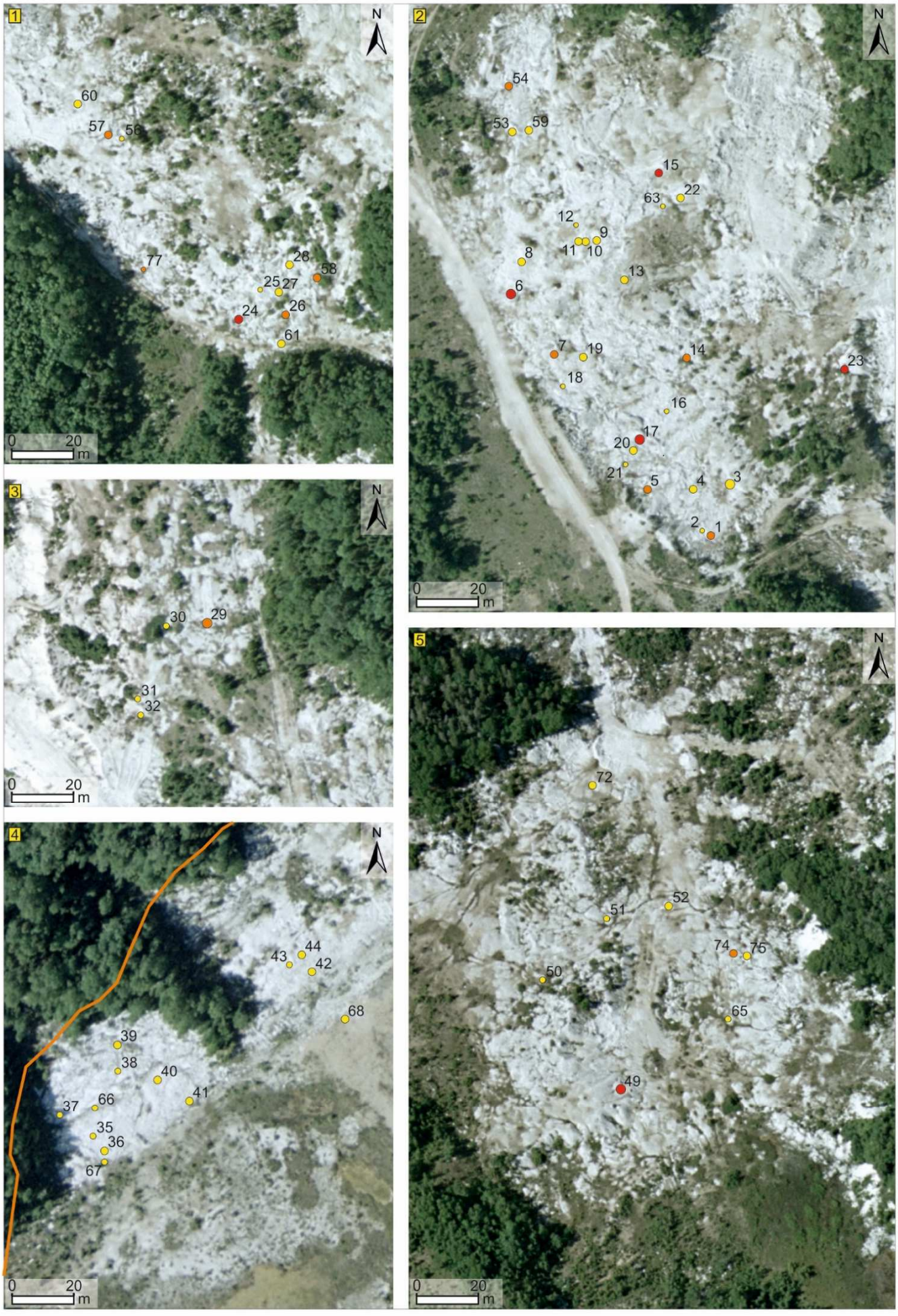

Supplementary material to the paper: Jarzyna A., Bąbel M., Ługowski D., Vladi F. 2022. Morphology of dome- and tepee-like landforms generated by expansive hydration of weathering anhydrite: a case study at Dingwall, Nova Scotia, Canada. In: Geomorphology in the Digital Era. A. Muzirafuti, G. Randazzo, S. Lanza (Eds.), Special Issue of Applied Sciences.

Figure S4

Location of hydration landforms with measured thickness of the detached layer on the basemap of satellite image (source: ArcGIS program).

Supplementary material to the paper: Jarzyna A., Bąbel M., Ługowski D., Vladi F. 2022. Morphology of dome- and tepee-like landforms generated by expansive hydration of weathering anhydrite: a case study at Dingwall, Nova Scotia, Canada. In: Geomorphology in the Digital Era. A. Muzirafuti, G. Randazzo, S. Lanza (Eds.), Special Issue of Applied Sciences.

Figure S5

Frequency distribution diagrams of morphometric parameters characterising hydration landforms, for intervals lef-closed and right-open.

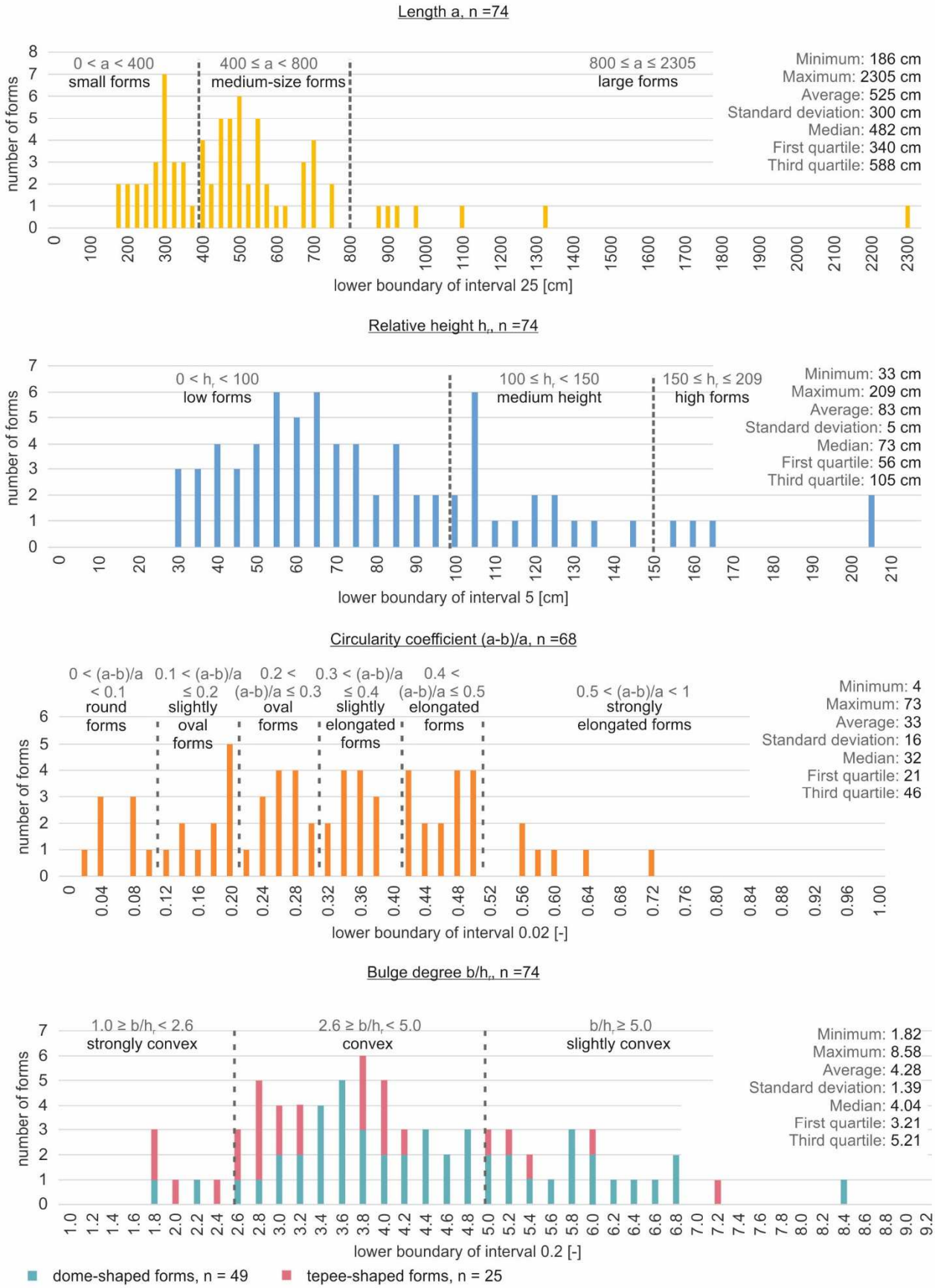

Supplementary material to the paper: Jarzyna A., Bąbel M., Ługowski D., Vladi F. 2022. Morphology of dome- and tepee-like landforms generated by expansive hydration of weathering anhydrite: a case study at Dingwall, Nova Scotia, Canada. In: Geomorphology in the Digital Era. A. Muzirafuti, G. Randazzo, S. Lanza (Eds.), Special Issue of Applied Sciences.

Figure S6

Dependence of relative height of hydration landforms on length, width, bulge degree and coefficient of circularity, taking into account classification of forms according to relative height.

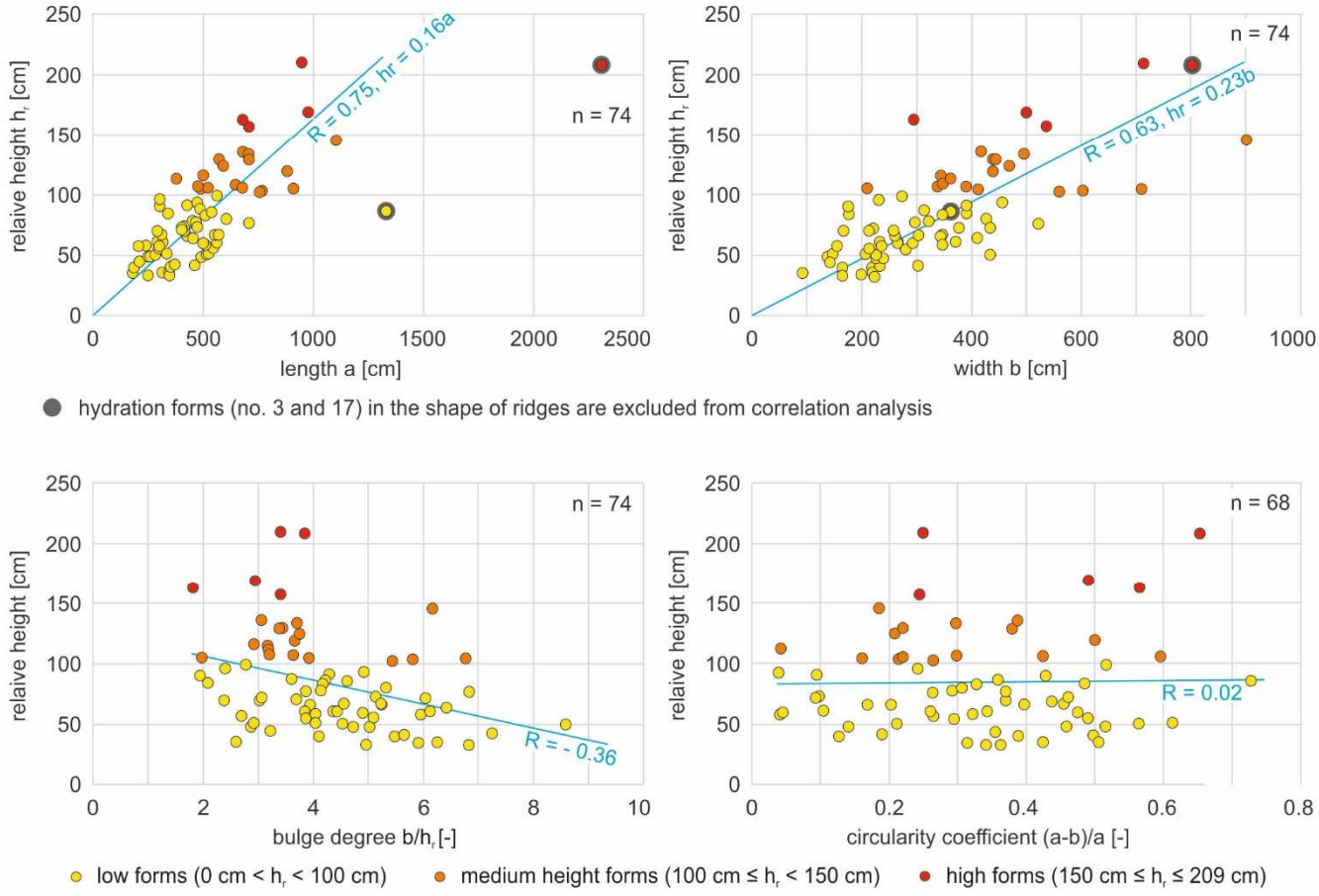

Supplementary material to the paper: Jarzyna A., Bąbel M., Ługowski D., Vladi F. 2022. Morphology of dome- and tepee-like landforms generated by expansive hydration of weathering anhydrite: a case study at Dingwall, Nova Scotia, Canada. In: Geomorphology in the Digital Era. A. Muzirafuti, G. Randazzo, S. Lanza (Eds.), Special Issue of Applied Sciences.

Figure S7

Pattern of fractures within hydration forms, with identifying no. and surface density of fractures given at the upper left (see Figure S3 for location of the forms); green circle marks place of the orthophotomap presented on the right.

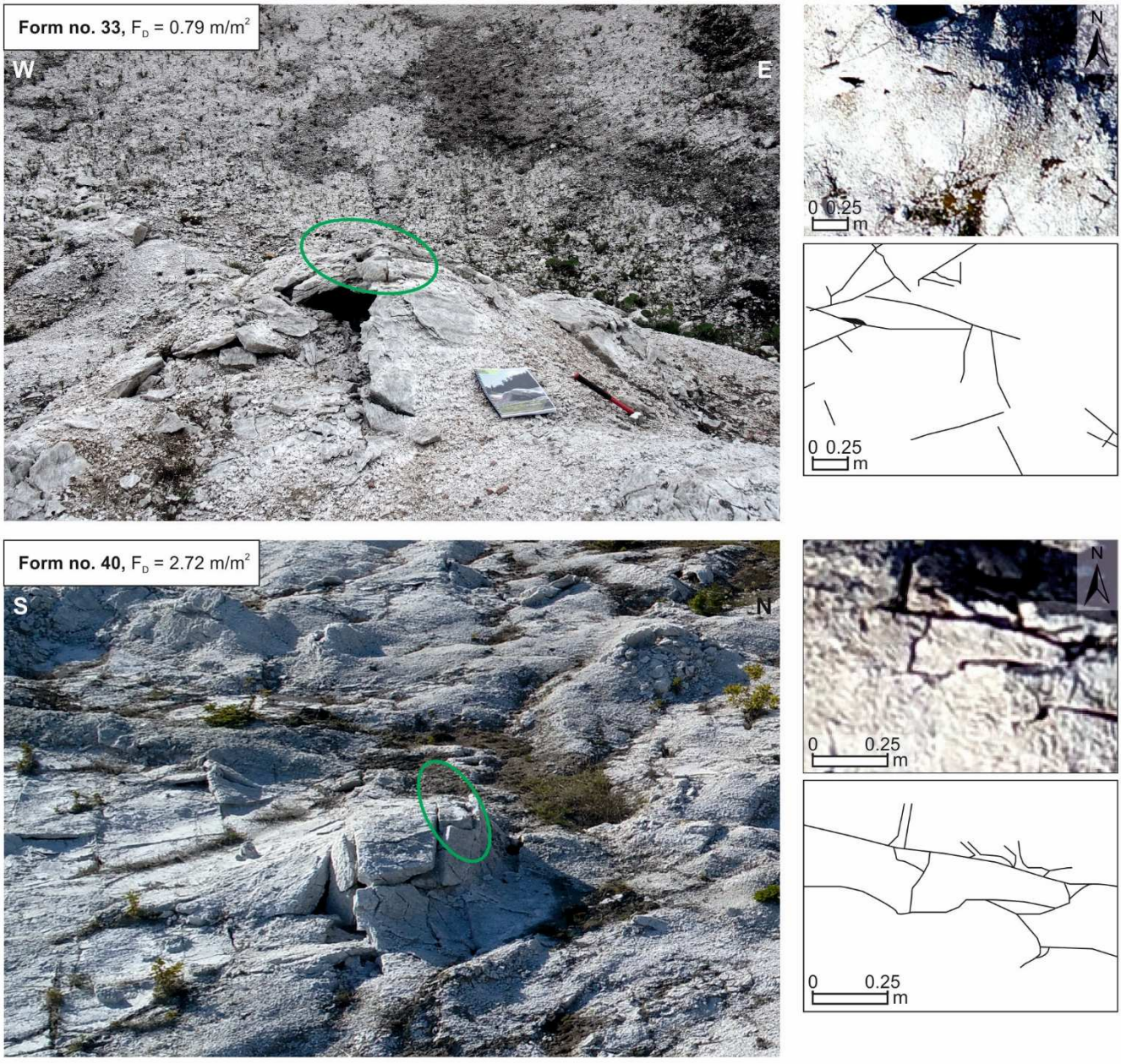

Supplementary material to the paper: Jarzyna A., Bąbel M., Ługowski D., Vladi F. 2022. Morphology of dome- and tepee-like landforms generated by expansive hydration of weathering anhydrite: a case study at Dingwall, Nova Scotia, Canada. In: Geomorphology in the Digital Era. A. Muzirafuti, G. Randazzo, S. Lanza (Eds.), Special Issue of Applied Sciences.

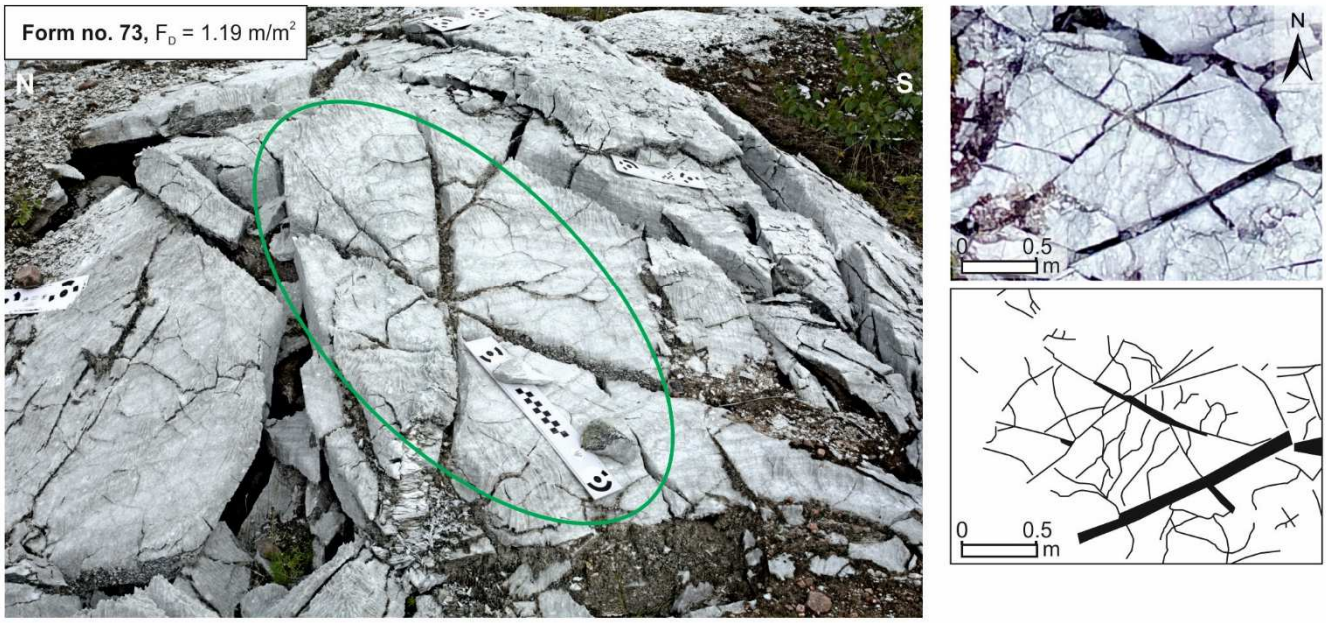

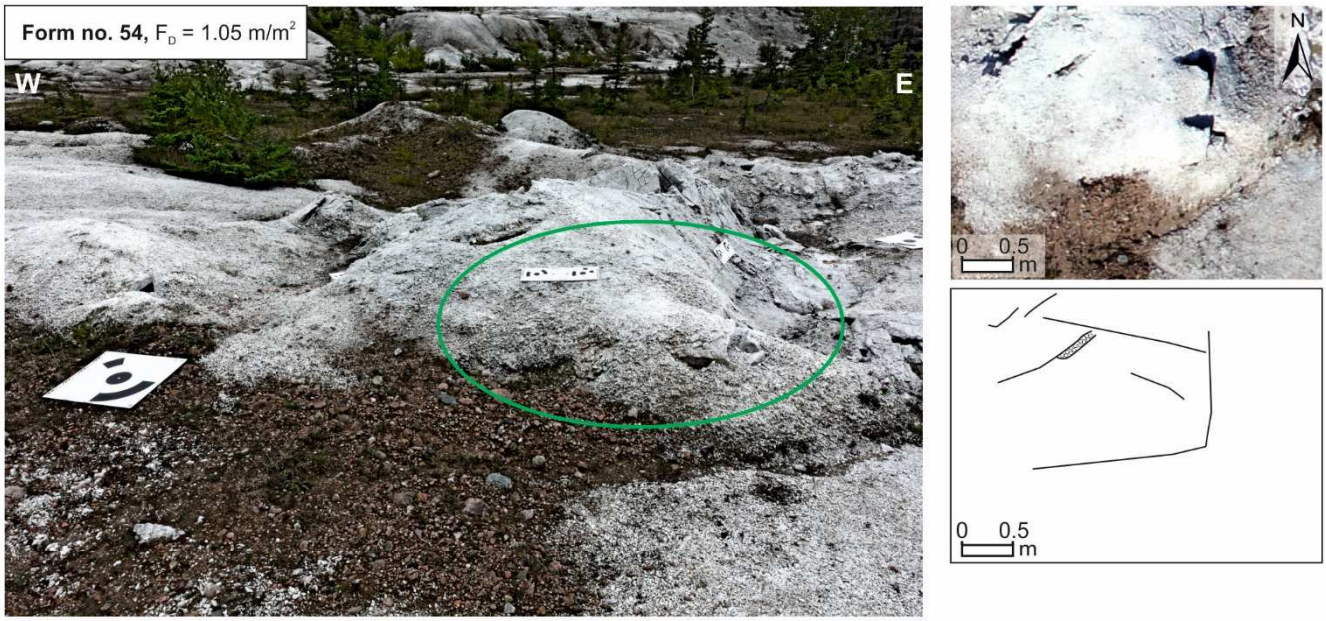

Supplementary material to the paper: Jarzyna A., Bąbel M., Ługowski D., Vladi F. 2022. Morphology of dome- and tepee-like landforms generated by expansive hydration of weathering anhydrite: a case study at Dingwall, Nova Scotia, Canada. In: Geomorphology in the Digital Era. A. Muzirafuti, G. Randazzo, S. Lanza (Eds.), Special Issue of Applied Sciences.

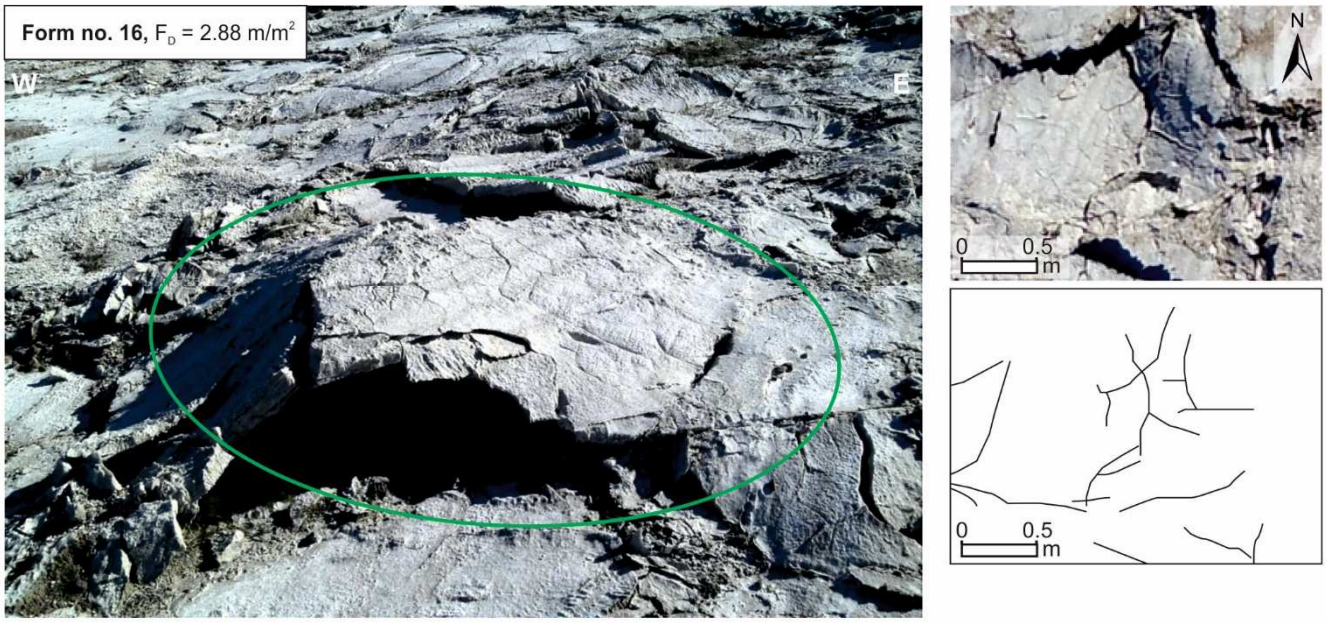

Supplementary material to the paper: Jarzyna A., Bąbel M., Ługowski D., Vladi F. 2022. Morphology of dome- and tepee-like landforms generated by expansive hydration of weathering anhydrite: a case study at Dingwall, Nova Scotia, Canada. In: Geomorphology in the Digital Era. A. Muzirafuti, G. Randazzo, S. Lanza (Eds.), Special Issue of Applied Sciences.

Figure S8

Traces of fractures and rock layers on the orthophotomaps of the quarry bottom and their rose diagrams (N – total number of fractures, L – total length of fractures, M – maximum length of a circle radius).

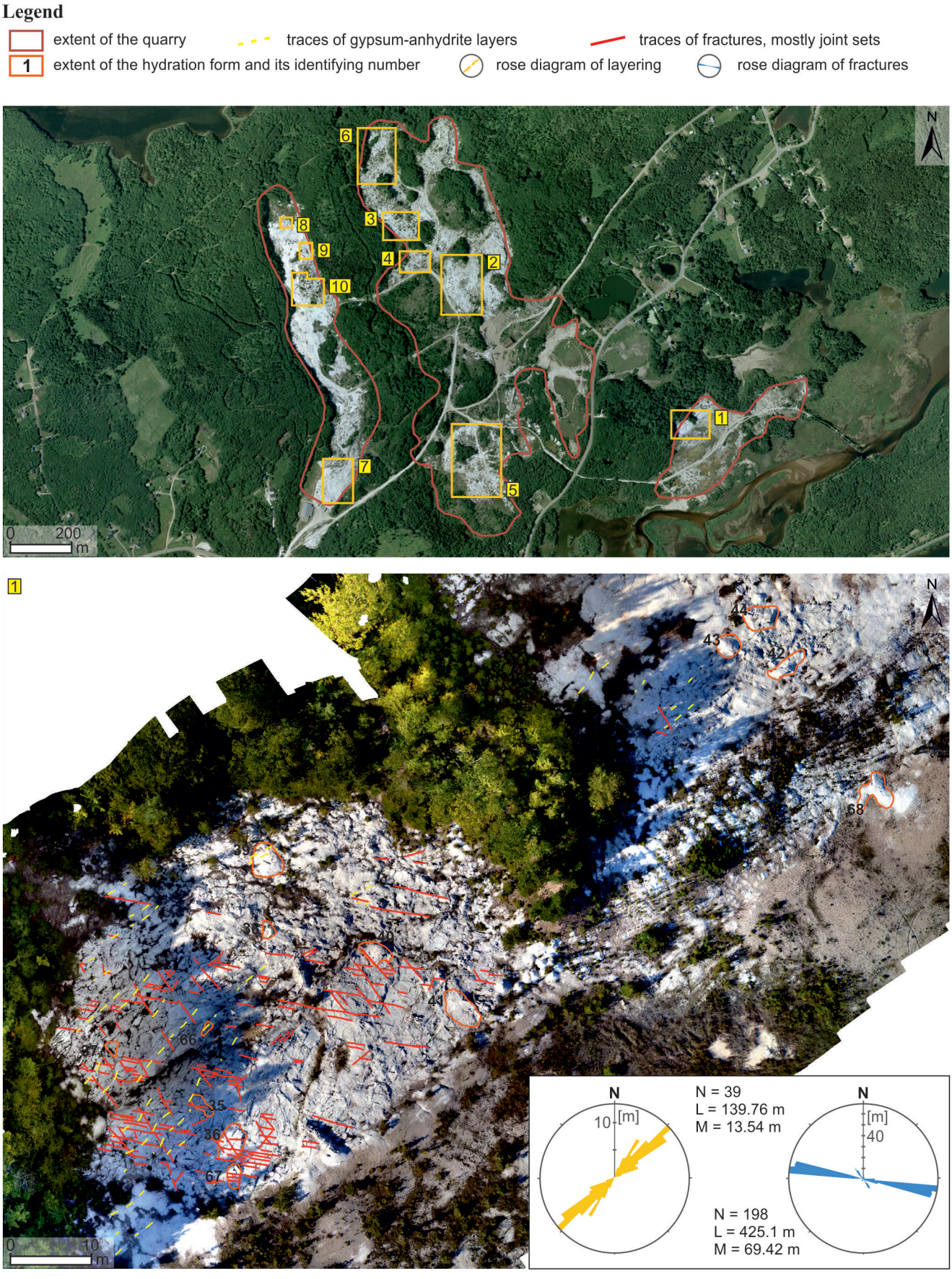

Supplementary material to the paper: Jarzyna A., Bąbel M., Ługowski D., Vladi F. 2022. Morphology of dome- and tepee-like landforms generated by expansive hydration of weathering anhydrite: a case study at Dingwall, Nova Scotia, Canada. In: Geomorphology in the Digital Era. A. Muzirafuti, G. Randazzo, S. Lanza (Eds.), Special Issue of Applied Sciences.

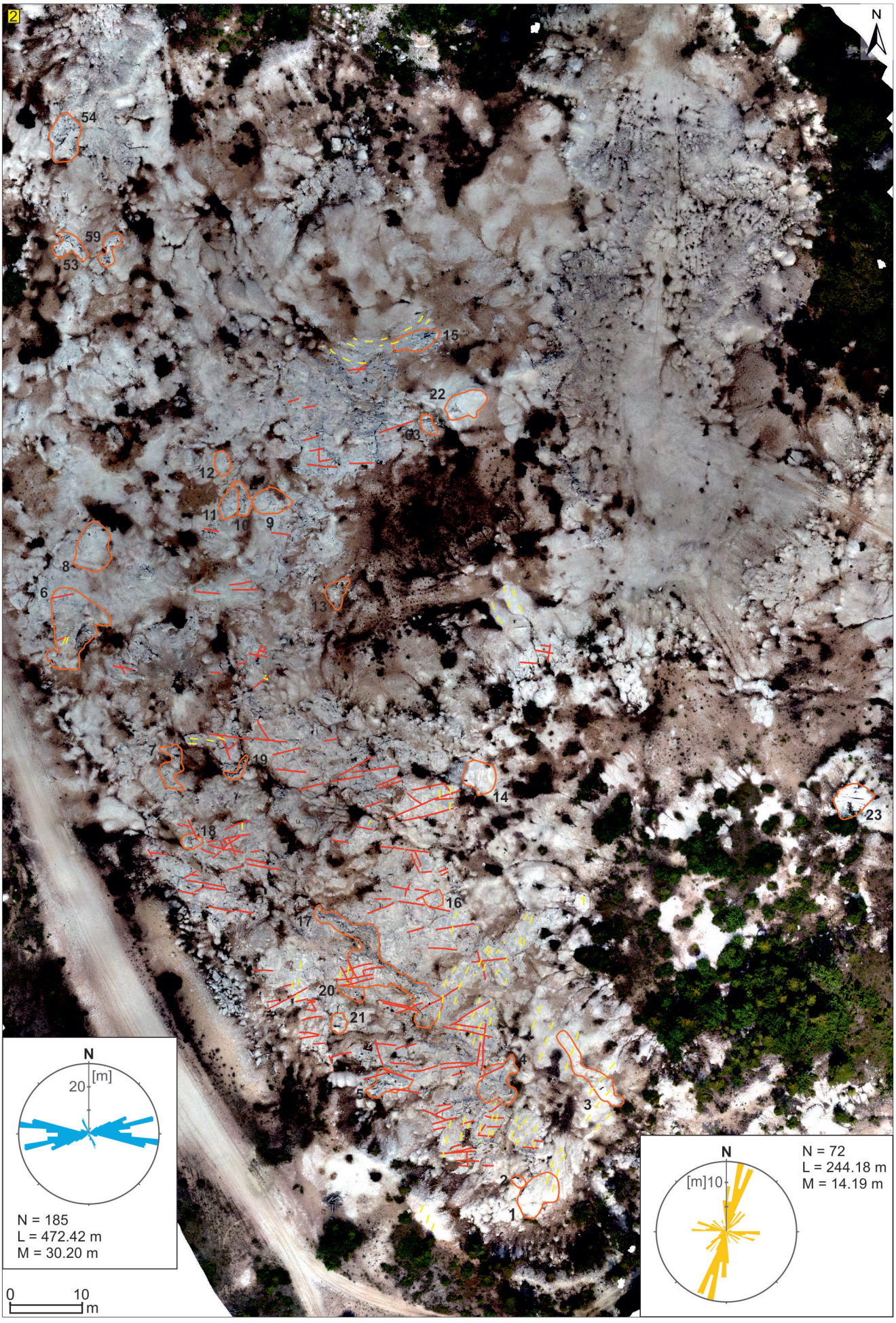

Supplementary material to the paper: Jarzyna A., Bąbel M., Ługowski D., Vladi F. 2022. Morphology of dome- and tepee-like landforms generated by expansive hydration of weathering anhydrite: a case study at Dingwall, Nova Scotia, Canada. In: Geomorphology in the Digital Era. A. Muzirafuti, G. Randazzo, S. Lanza (Eds.), Special Issue of Applied Sciences.

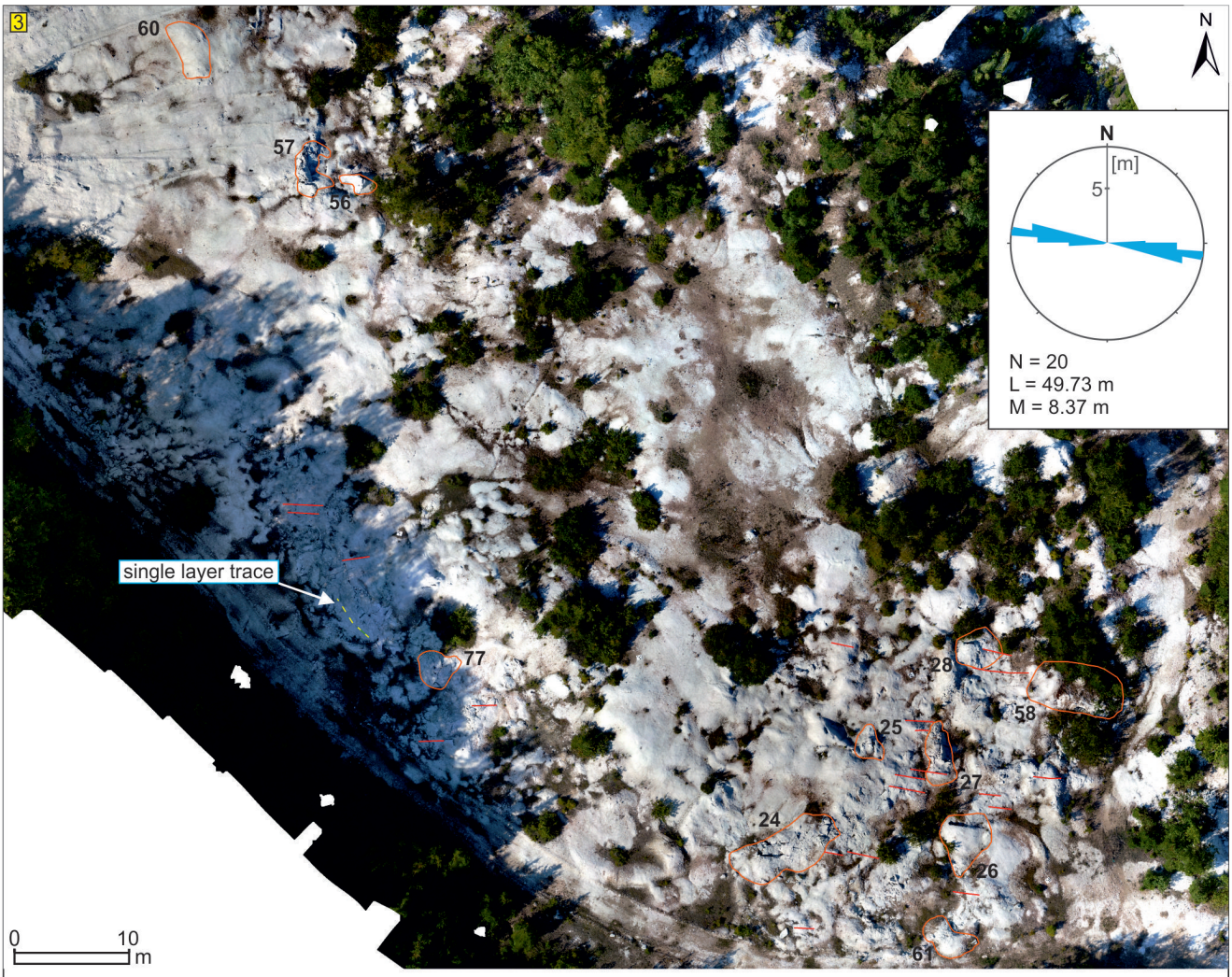

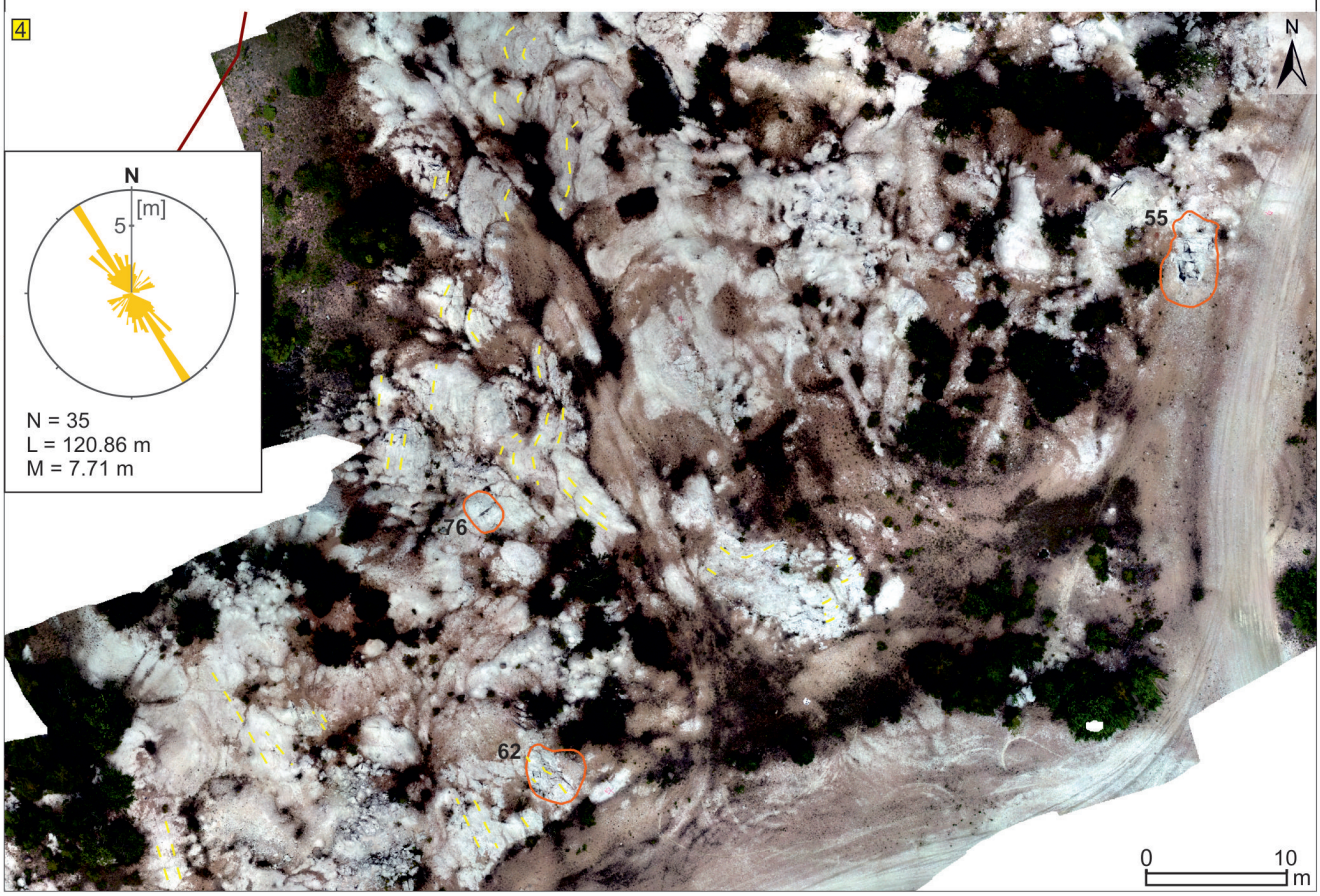

Supplementary material to the paper: Jarzyna A., Bąbel M., Ługowski D., Vladi F. 2022. Morphology of dome- and tepee-like landforms generated by expansive hydration of weathering anhydrite: a case study at Dingwall, Nova Scotia, Canada. In: Geomorphology in the Digital Era. A. Muzirafuti, G. Randazzo, S. Lanza (Eds.), Special Issue of Applied Sciences.

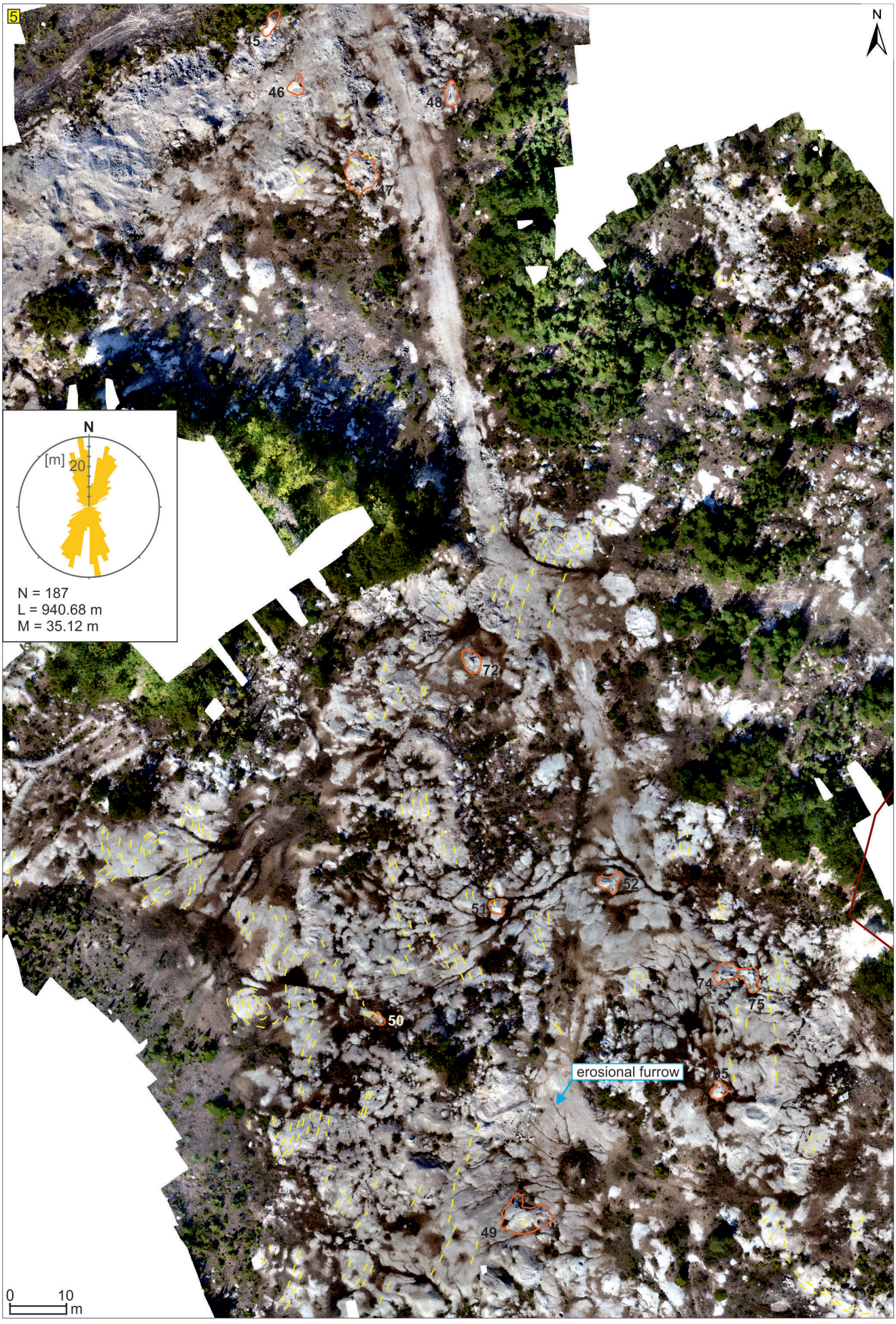

Supplementary material to the paper: Jarzyna A., Bąbel M., Ługowski D., Vladi F. 2022. Morphology of dome- and tepee-like landforms generated by expansive hydration of weathering anhydrite: a case study at Dingwall, Nova Scotia, Canada. In: Geomorphology in the Digital Era. A. Muzirafuti, G. Randazzo, S. Lanza (Eds.), Special Issue of Applied Sciences.

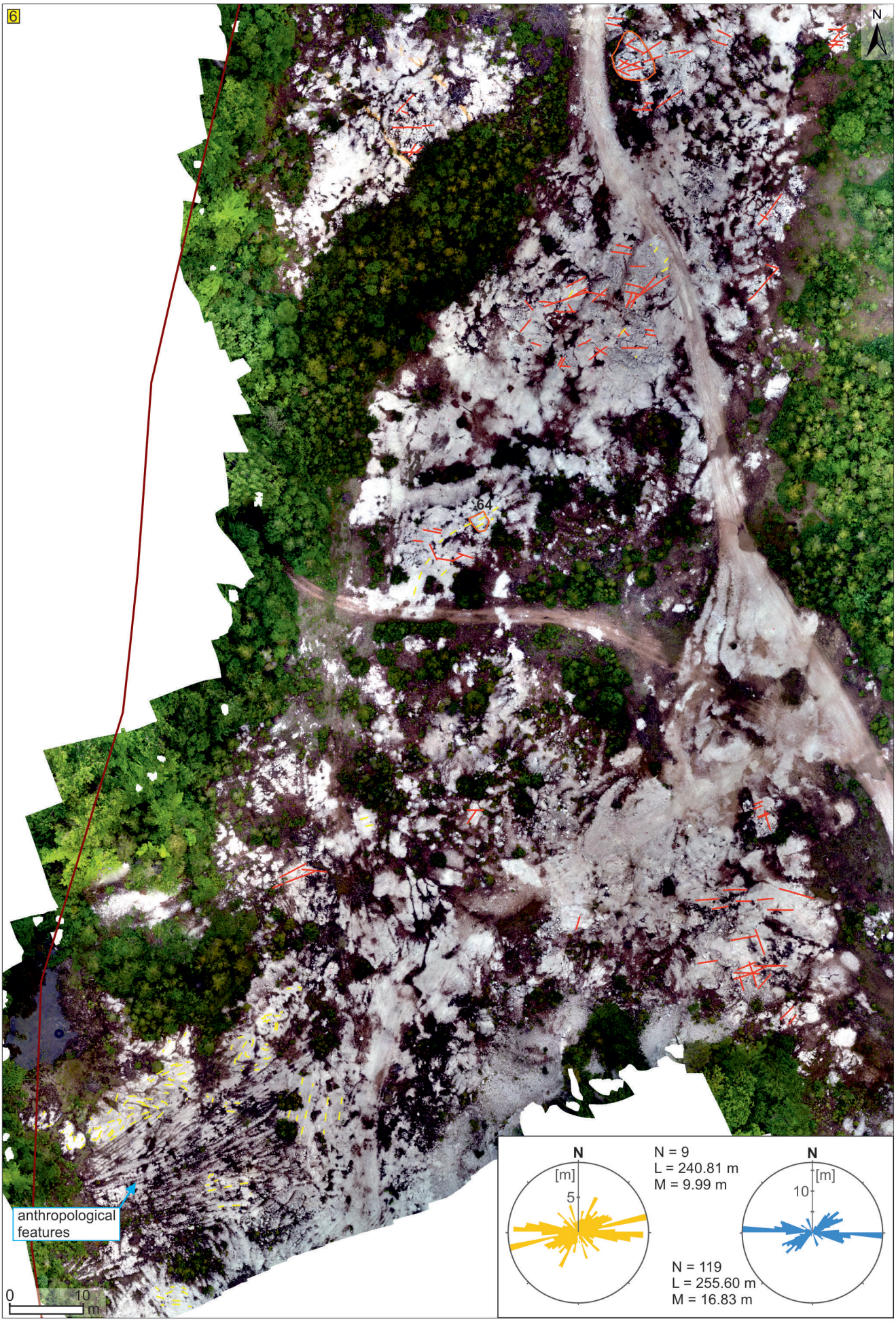

Supplementary material to the paper: Jarzyna A., Bąbel M., Ługowski D., Vladi F. 2022. Morphology of dome- and tepee-like landforms generated by expansive hydration of weathering anhydrite: a case study at Dingwall, Nova Scotia, Canada. In: Geomorphology in the Digital Era. A. Muzirafuti, G. Randazzo, S. Lanza (Eds.), Special Issue of Applied Sciences.

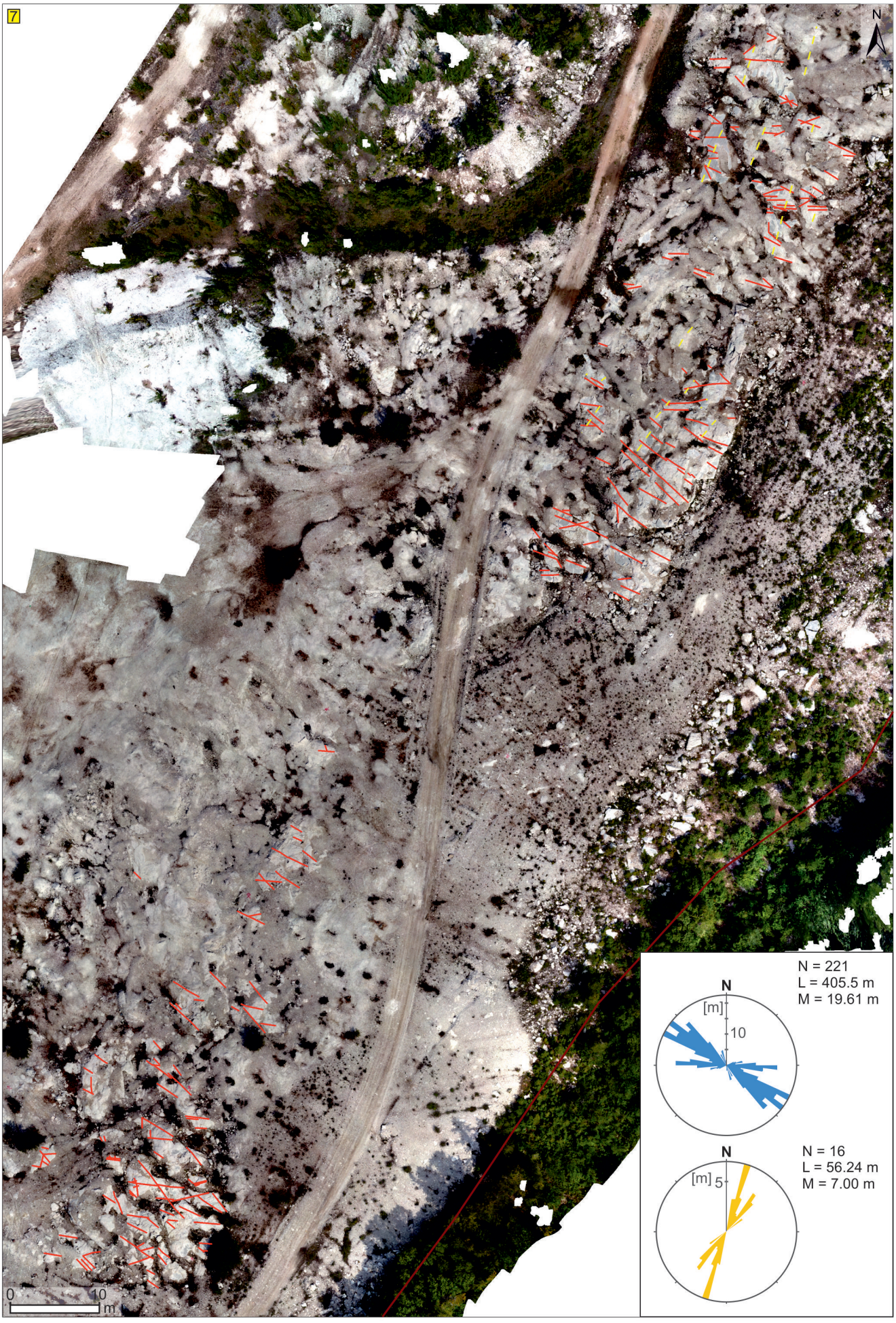

Supplementary material to the paper: Jarzyna A., Bąbel M., Ługowski D., Vladi F. 2022. Morphology of dome- and tepee-like landforms generated by expansive hydration of weathering anhydrite: a case study at Dingwall, Nova Scotia, Canada. In: Geomorphology in the Digital Era. A. Muzirafuti, G. Randazzo, S. Lanza (Eds.), Special Issue of Applied Sciences.

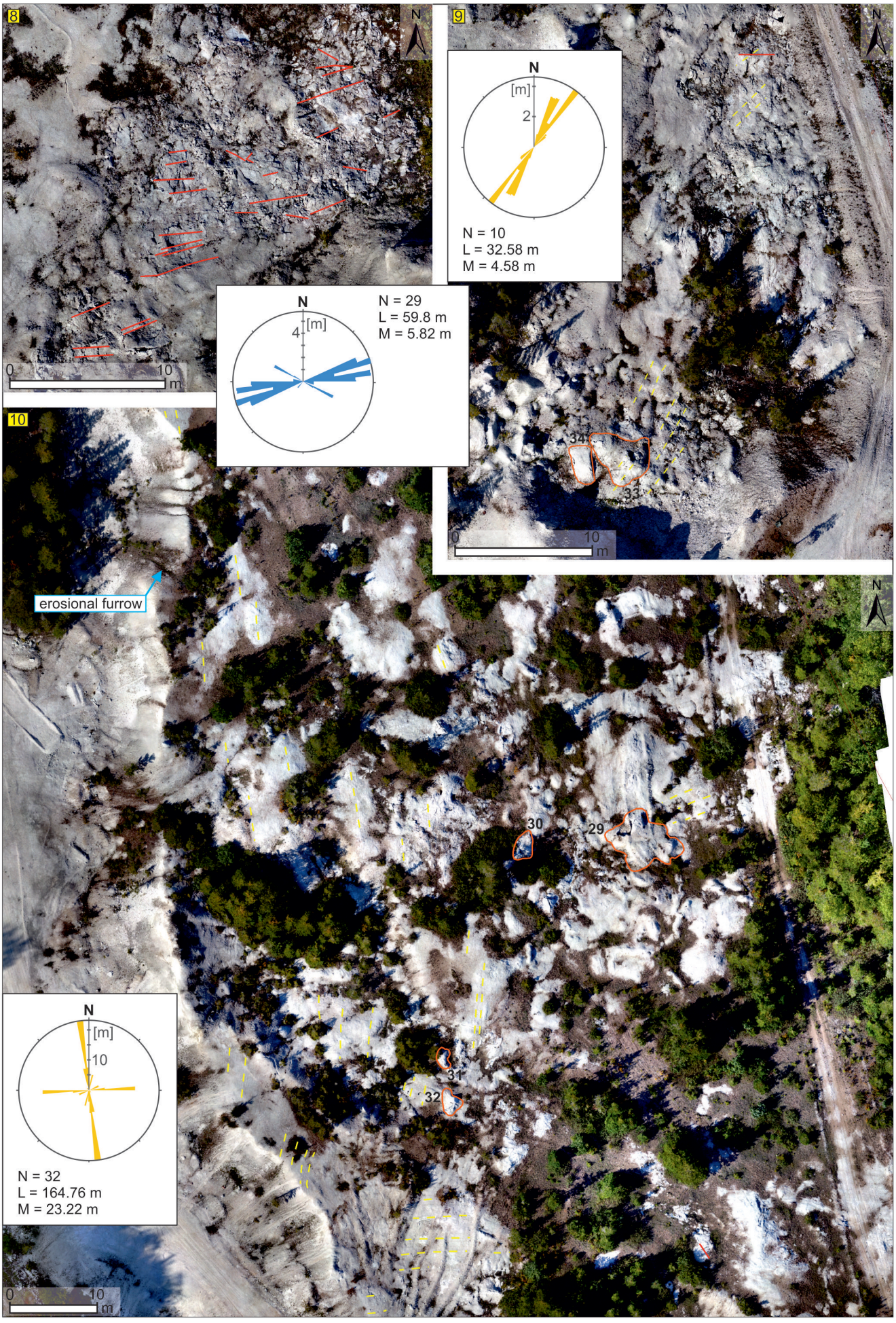

Supplementary material to the paper: Jarzyna A., Bąbel M., Ługowski D., Vladi F. 2022. Morphology of dome- and tepee-like landforms generated by expansive hydration of weathering anhydrite: a case study at Dingwall, Nova Scotia, Canada. In: Geomorphology in the Digital Era. A. Muzirafuti, G. Randazzo, S. Lanza (Eds.), Special Issue of Applied Sciences.

Figure S9

Exemplary hydration landforms influenced by structural types of bedrock.

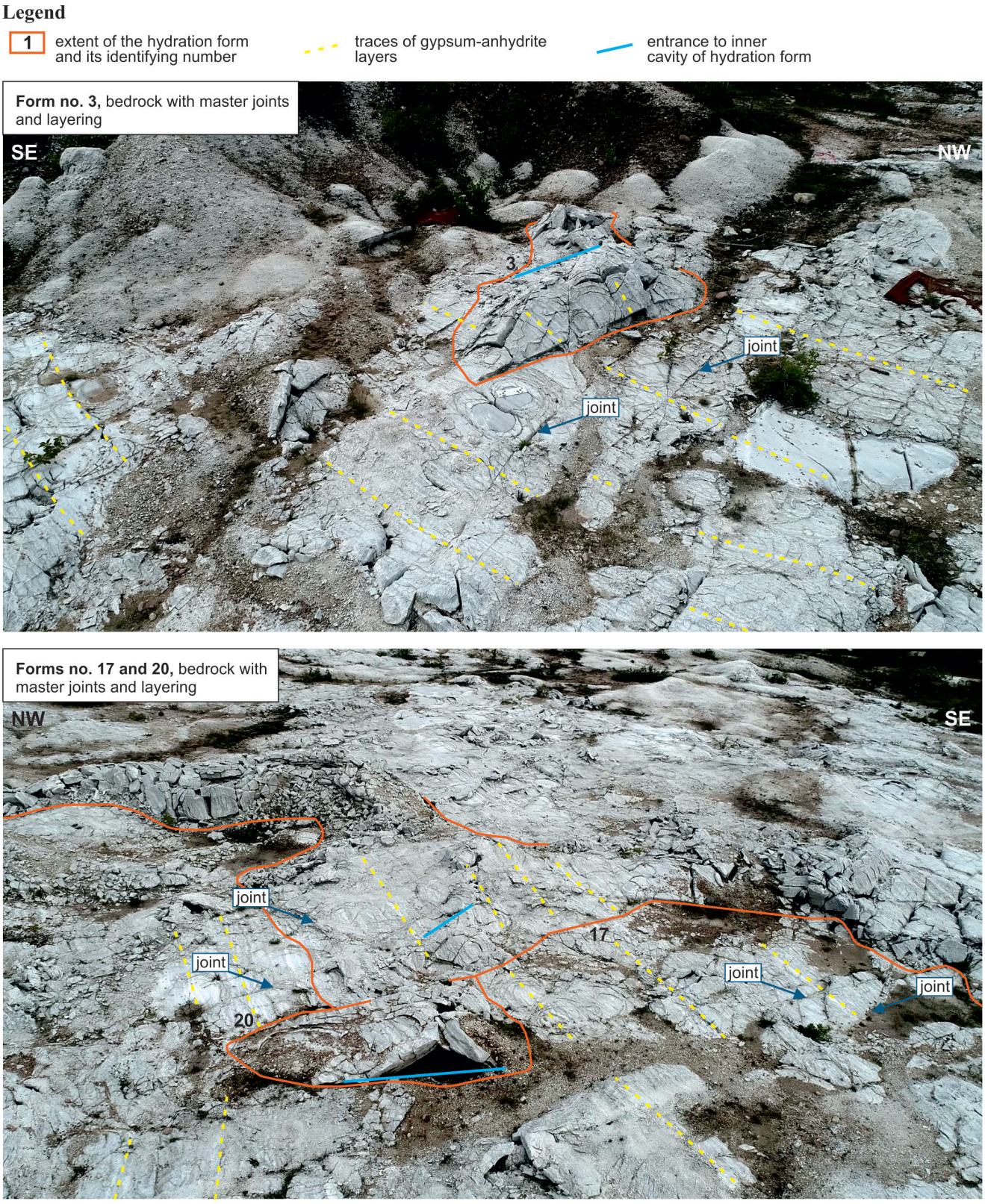
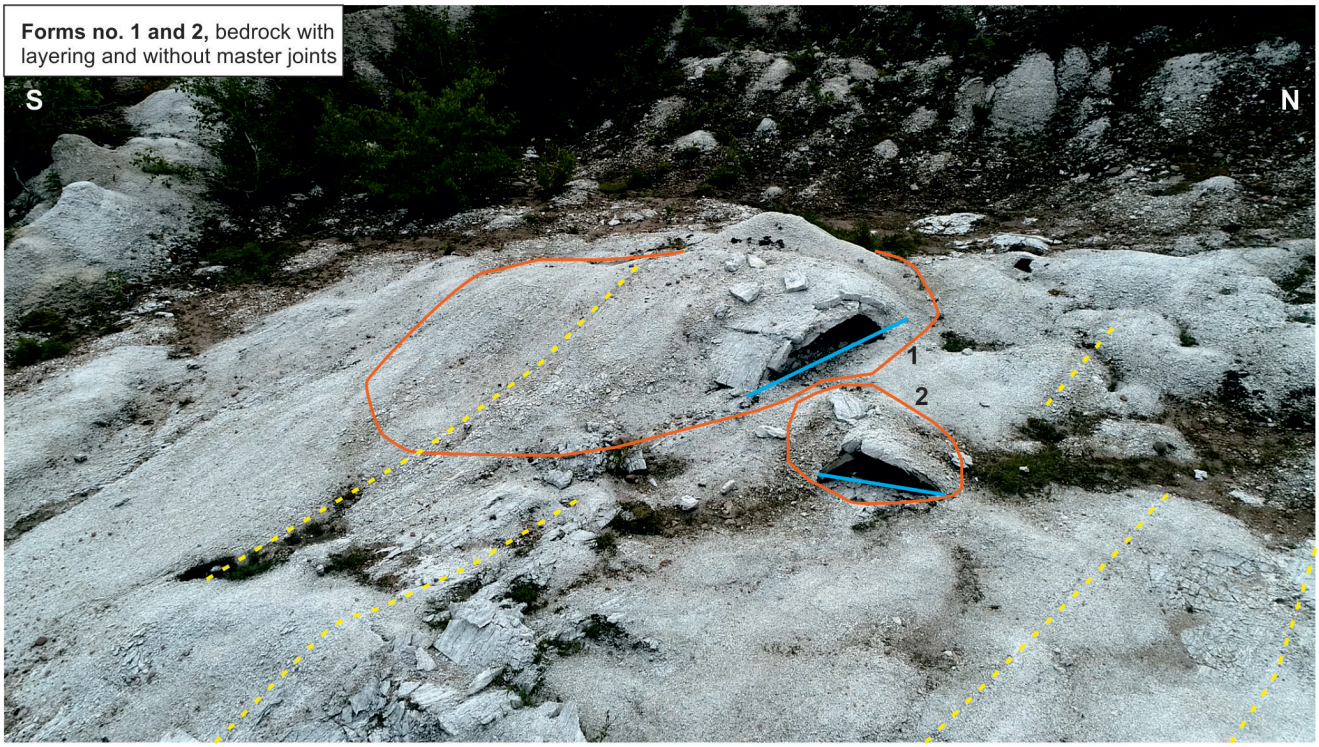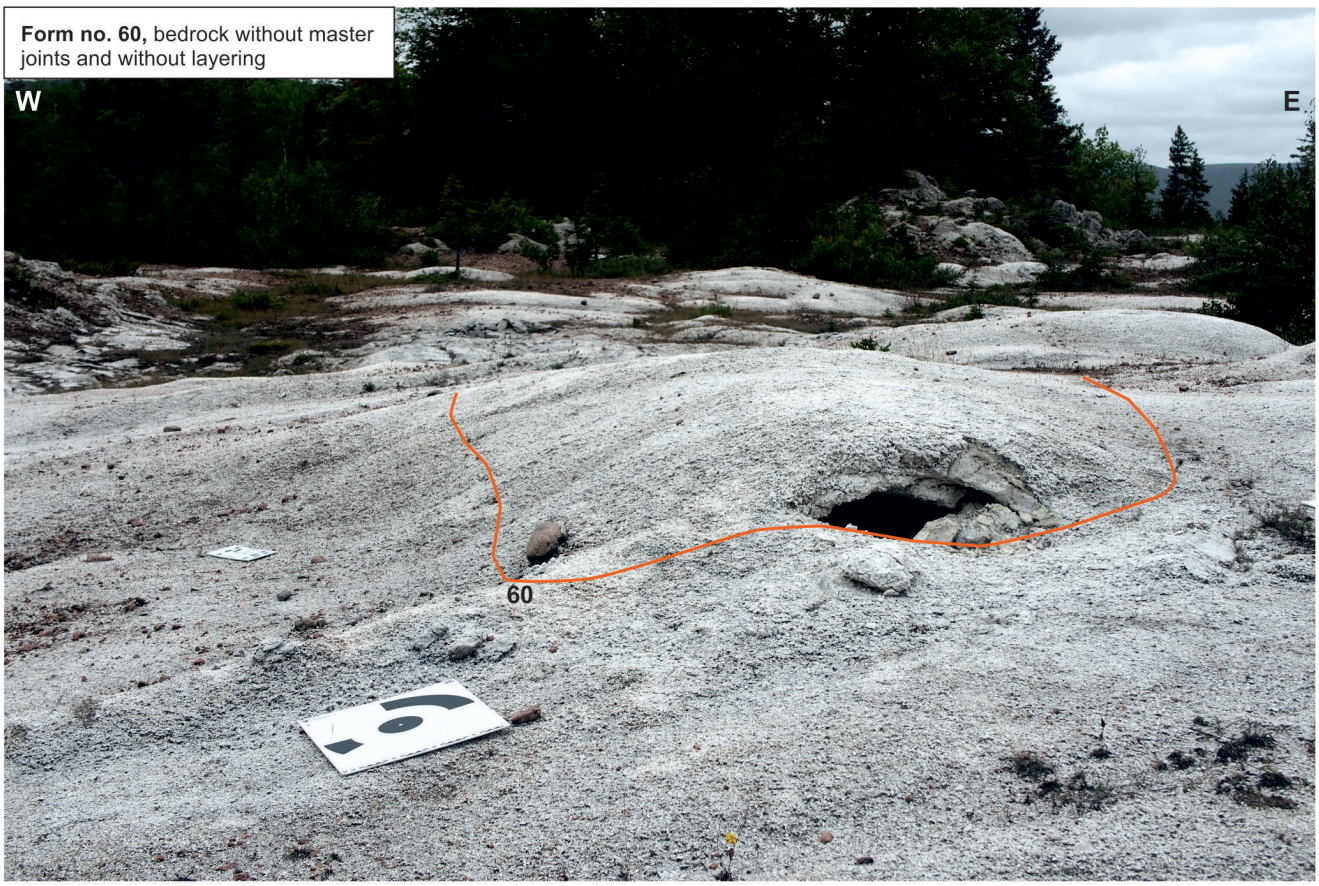
Supplementary material to the paper: Jarzyna A., Bąbel M., Ługowski D., Vladi F. 2022. Morphology of dome- and tepee-like landforms generated by expansive hydration of weathering anhydrite: a case study at Dingwall, Nova Scotia, Canada. In: Geomorphology in the Digital Era. A. Muzirafuti, G. Randazzo, S. Lanza (Eds.), Special Issue of Applied Sciences.